Growth of Necrotic Tumours in the Presence and Absence of Inhibitors

H.M. Byrne & M.A.J. Chaplain
School of Mathematical Sciences
University of Bath
Claverton Down
Bath BA2 7AY
Telephone: 44 01225 826242
Fax: 01225 826492
e-mail: hmb, majc@maths.bath.ac.uk

Abstract

In this paper we present a mathematical model for the growth of a multicellular spheroid which comprises a central core of necrotic cells, surrounded by an outer annulus of proliferating cells. The model distinguishes between two mechanisms for cell loss: apoptosis and necrosis. Cell loss due to apoptosis is programmed cell death, occurring, for example, when a cell exceeds its natural lifespan, whereas cell death due to necrosis is induced by changes in the cell's microenvironment, occurring, for example, in nutrient-depleted regions. Mathematically, the problem involves tracking two free boundaries, one for the outer tumour radius, the other for the inner necrotic radius. Numerical simulations of the model are presented in an inhibitor-free setting and an inhibitor-present setting for various parameter values. The effects of nutrients and inhibitors on the existence and stability of the time-independent solutions of the model are also studied using a combination of numerical and asymptotic techniques.

Submitted to Mathematical Biosciences June 29, 1995

1. Introduction

In vivo cancer growth is a complicated phenomenon involving many inter-related processes and correspondingly the mathematical modelling of such problems is very difficult. However, over the past twenty years an increasing number of mathematical models describing solid tumour growth (or multicellular spheroid growth) have appeared in the literature [1], [2], [3], [4], [5]. Typically, such models regard the tumour as a growing spherical mass of cells whose internal architecture consists of a layer of proliferating cells surrounding a necrotic core. A third, intermediate region of quiescent cells is also sometimes included. Analysis of such models enables the relative importance of the different mechanisms involved in the growth process to be examined and may also assist in assessing the relative merits of different courses of drug treatment or chemotherapy [6], [7], [8], [9], [10], [11], [12]. Many of the existing deterministic tumour models consist of an ordinary differential equation, coupled to one, or more, reaction-diffusion equations. The ordinary differential equation derives from mass conservation applied to the tumour and describes the evolution of the tumour boundary, whereas the reaction-diffusion equations describe the distribution, within the tissue, of nutrients, such as oxygen and glucose, and growth inhibitory factors (GIFs), such as chalones [13], [14], [15].

In an earlier paper [16] we considered the evolution of a single tumour prior to the onset of necrosis and examined the effects of externally supplied nutrients and inhibitors on the existence and stability of radially-symmetric, time-independent (non-necrotic) solutions. Here this work is extended to include the simplest heterogeneous tumour configuration which comprises a central necrotic core and an outer layer of proliferating cells. Both models provide insight into the action of a number of different inhibitor mechanisms. In particular, the inhibitor can be regarded as either an anti-cancer drug or a naturally-occurring inhibitor, stimulated by the immune system in response to the foreign body. In [16] we showed that, with no inhibitor present, nontrivial solutions exist, and are stable, for a range of the system parameters which corresponds to a balance between cell proliferation and natural cell death, or apoptosis [17], [18]. In addition, where no nontrivial solutions exist, the trivial, tumour-free solution is stable. By permitting the existence of tumours which possess a central necrotic core, in this paper we are able to extend the range of parameters for which nontrivial solutions exist and also to distinguish between apoptosis and necrosis as distinct cell loss mechanisms. As mentioned above, apoptosis describes natural, or programmed, cell death caused, for example, by aging of the tumour cells. By contrast, necrosis describes cell death which is triggered by the microenvironment when, for example, the local nutrient concentration is insufficient to sustain an individual cell.

Once again for simplicity of exposition, a single nutrient species and a single inhibitor species are considered, so that the model comprises two coupled reaction-diffusion equations, one for each species, an integro-differential equation, which describes the evolution of the outer tumour boundary, and a further equation which implicitly defines the evolution of the boundary of the necrotic core. In the following sections we use a combination of numerical and analytical techniques to investigate how the growth of a radially symmetric tumour can be influenced by different types of nutrients and inhibitors. Several results are derived which could be validated with experimental data. For example, we show that, when no inhibitor is present and the necrotic core is small, changes in the necrotic radius occur much more rapidly and on a larger scale than changes in the outer tumour radius, the balance between the rate of apoptosis and the nutrient concentration at which necrosis commences determining whether growth or regression of the tumour ensues: the rate of cell degradation due to necrosis does not affect this result. Necessary conditions for the existence of tumours which possess the thin proliferating rim frequently observed *in vitro* are also derived. In order to obtain tumours which possess a thin proliferating rim the external nutrient concentration (σ_∞) should be only slightly larger than the concentration at which necrosis is initiated (σ_{nec}) and the rate of necrosis should be sufficiently small. In this case, the dependence of the width of the proliferating rim on σ_∞ and σ_{nec} agrees with the expression *assumed* by Greenspan [4]. Modifications to a tumour's growth characteristics brought about by the presence of different types of inhibitors are also investigated and shown to have significant effect in certain cases. The implications of these results for the development and treatment of cancer are also discussed.

2. The Mathematical Model

The mathematical model studied here describes the evolution of a spherically symmetric, multicellular spheroid. The centre, or necrotic core, of the tumour contains only dead cells and has radius $r_{in}(t)$ whilst the outer, proliferating rim contains rapidly dividing cells and has radius $R(t)$. The model focusses on a single, externally supplied nutrient, such as glucose or oxygen, and also a growth-inhibitory species. The inhibitor may be regarded as either an anti-cancer drug or a chemical produced in vivo as part of the host's immune response to the foreign body. We examine the effect that these chemicals have on the subsequent development of the tumour.

The model comprises two reaction-diffusion equations, describing the evolution of the nutrient and inhibitor species, and an integro-differential equation, governing the evolution of the tumour's outer radius, $R(t)$. The necrotic radius $r_{in}(t)$ is defined implicitly, occurring where the nutrient concentration (σ) attains a specified value, σ_{nec} say, and such that there is cell proliferation where $\sigma > \sigma_{nec}$ and cell death where $\sigma < \sigma_{nec}$.

Now, there are two natural timescales associated with tumour growth, the first related to the growth rate of the tissue and the second related to nutrient diffusion. Given that a tumour may expand at a rate of up to 0.5 mm/day and that a typical diffusion timescale is 1 min ($\equiv L^2/D$, where $L \sim 10^{-2}$ cm is a typical length scale and $D \sim 10^{-6}$ cm^2 s^{-1} a typical diffusion coefficient), it is clear that the diffusion timescale of nutrients and inhibitors is much shorter than the growth timescale. Thus, as the tumour grows, the nutrient and inhibitor rapidly redistribute themselves to occupy the new tumour volume. Following , [1], [4], [19] we exploit this difference by focussing on the longer, growth timescale and adopt a quasi-steady approach, with $\partial/\partial t \equiv 0$ in the governing reaction-diffusion equations. Further, since the necrotic core contains only dead cells, we assume that species in that region are subject solely to diffusional effects: any nutrient/inhibitor reaction terms are identically zero there. Denoting by $H(.)$ the Heaviside step-function ($H(x) = 1$ if $x > 0$, $H(x) = 0$ if $x \leq 0$), and restricting attention to spherically-symmetric polar coordinates, the following reaction-diffusion equations, valid for $r \in [0, R]$, determine the nutrient (σ) and inhibitor (β) species:

$$0 = \frac{D_1}{r^2}\frac{\partial}{\partial r}\left(r^2\frac{\partial \sigma}{\partial r}\right) - \Gamma\sigma H(r - r_{in}) - g_1(\sigma,\beta)H(r - r_{in}), \tag{2.1}$$

$$0 = \frac{D_2}{r^2}\frac{\partial}{\partial r}\left(r^2\frac{\partial \beta}{\partial r}\right) - g_2(\sigma,\beta)H(r - r_{in}), \tag{2.2}$$

where $D_i (i = 1, 2)$ are the assumed constant nutrient and inhibitor diffusion coefficients, Γ describes the rate at which proliferating cells consume the nutrient in the absence of any inhibitor. The reaction rate $g_1(\sigma, \beta)$ describes the manner in which the inhibitor depletes the available nutrients whilst $g_2(\sigma, \beta)$ describes the inhibitor's decay. (Functional forms for $g_i(\sigma, \beta)(i = 1, 2)$ are discussed below.) Whilst no time-derivatives appear in (2.1)-(2.2), the intrinsic dependence of σ and β on $R(t)$ and $r_{in}(t)$ governs their evolution as the tumour develops.

Now, the growth rate of the tumour is dependent on the number of proliferating cells contained inside it. Assuming that this active cell density is directly related to the nutrient concentration, henceforth, no explicit mention is made of the cell density inside the tumour, some function of the nutrient concentration replacing it instead. Since cell proliferation is confined to the annulus $r_{in} < r < R$, and the proliferation rate may depend on the inhibitor concentration, we denote by $S(\sigma, \beta) = \bar{S}(\sigma, \beta)H(r - r_{in})$ the proliferation rate at a point inside the tumour. For $0 < r < r_{in}$ the microenvironment is nutrient-depleted $(\sigma < \sigma_{nec})$ and unable to support proliferating cells. Cells within this region undergo necrosis: that is, they die and are continuously degraded, forming smaller molecules which diffuse easily out of the tumour. This microenvironment-induced effect is incorporated by assuming a constant volume loss term ($\equiv 3\lambda$) at all points inside the necrotic core. Mass conservation then yields the following equation which describes the evolution of the outer tumour radius $R(t)$:

$$
\begin{aligned}
\frac{d}{dt}\left(\frac{4}{3}\pi R^3\right) &= \int_{tumour} S(\sigma, \beta) r^2 \sin\theta dr d\theta d\phi, \\
\Rightarrow \frac{dR}{dt} &= \frac{1}{R^2}\left\{\int_{r_{in}(t)}^{R(t)} \bar{S}(\sigma, \beta) r^2 dr - \lambda r_{in}^3\right\}. \qquad (2.3)
\end{aligned}
$$

We assume that the cell proliferation rate $S(\sigma, \beta)$ is a balance between the creation, or birth, of cells, and apoptosis, or programmed cell death (see [20], [17], [18], [12] for a description of the structural changes involved in apoptosis). We define the key difference between apoptosis and necrosis as cell loss mechanisms as follows: necrosis is induced by the external microenvironment whereas apoptosis is an intrinsic property of a cell Thus, insufficient nutrient levels may trigger cell death due to necrosis whilst, if a cell lives beyond its finite lifespan, then cell death due to apoptosis may result. The inclusion of apoptosis as a cell loss mechanism distinguishes this work from that of, for example, , [4], [5]. Motivation for the inclusion of such a term stems from the existence of dormant tumour states [12]. Greenspan modelled this cell loss as a pressure gradient driven migration of cells from the tumour's outer rim to the necrotic core where they disintegrate into highly permeable waste products [4]. However, Durand's observations [20], [21] of only a small proportion of labelled nuclei in the necrotic core of a spheroid labelled with tritiated thymidine, a marker of DNA, strongly suggest that other cell loss mechanisms may occur. Other experiments support this view. Sutherland and Durand [9] observed no increase in the size of non-necrotic multicellular spheroids undergoing starvation. Further, Kerr *et al.* [17], [18] found that apoptosis can always be detected in neoplasms. In conclusion, it is highly likely that apoptosis is the cause of the observed volume loss in solid spheroids and should, therefore, be included in any mathematical model describing their evolution. To date, only McElwain and Morris [19] and Byrne and Chaplain [16] (see introduction) have incorporated apoptosis into a mathematical model. Assuming a constant cell (or, equivalently, nutrient) loss rate in mitosing regions, the model presented in [19] admits nontrivial steady solutions which have a two-layer structure: an outer, proliferating rim, enveloping a layer where the rates of nutrient consumption and cell proliferation fall.

Following [16] and to simplify the analysis, throughout this paper attention is focussed on a proliferation rate which is linear with respect to both nutrient and inhibitor concentrations. Thus we consider

$$\bar{S}(\sigma, \beta) = s(\sigma - \tilde{\sigma})(1 - \beta/\tilde{\beta}), \tag{2.4}$$

where $s, \tilde{\sigma}, \tilde{\beta}$ are constants. Whilst other choices for $\bar{S}(\sigma, \beta)$ could be studied, the resulting models generally require numerical solution and are, therefore, not considered here.

In order to close the system of equations defined by (2.1)–(2.3) boundary and initial conditions are now introduced. Symmetry of the tumour leads to the prescription of zero nutrient and inhibitor flux at $r = 0$. In addition, we assume that the nutrient and inhibitor concentrations are maintained at the constant values σ_∞ and β_∞ on $r = R(t)$. Continuity of $\sigma, \partial\sigma/\partial r, \beta, \partial\beta/\partial r$ is imposed across the necrotic boundary $r = r_{in}(t)$. The position of the necrotic boundary is defined implicitly, occurring where the nutrient concentration attains a specified value $\sigma = \sigma_{nec}$, and such that in the nutrient-rich microenvironment, where $\sigma > \sigma_{nec}$, tumour cells proliferate whereas in the nutrient-depleted microenvironment, where $\sigma < \sigma_{nec}$, cells become necrotic and die. Finally, the initial tumour radius $R(t = 0) = R_0$ is prescribed. In summary, the following boundary and initial conditions are imposed:

$$\frac{\partial \sigma}{\partial r} = 0 = \frac{\partial \beta}{\partial r} \quad \text{on} \quad r = 0, \tag{2.5}$$

$$\sigma = \sigma_\infty, \quad \beta = \beta_\infty, \quad \text{on} \quad r = R(t), \tag{2.6}$$

$$\sigma, \frac{\partial \sigma}{\partial r}, \beta, \frac{\partial \beta}{\partial r} \quad \text{continuous across} \quad r = r_{in}(t), \tag{2.7}$$

$$\sigma = \sigma_{nec} \quad \text{on} \quad r = r_{in}(t), \tag{2.8}$$

$$R(t = 0) = R_0, \quad \text{prescribed}. \tag{2.9}$$

Many authors have studied similar models of tumour growth, deriving necessary conditions for the appearance of a necrotic core [22], [4], [23]. However, our interest in studying the effect of inhibitors on the growth of tumours leads us to start from an initial, well-developed configuration, in which a necrotic core already exists.

Functional forms for the interaction terms g_1, g_2 in equations (2.1) and (2.2) are now considered, with a view to determining how different inhibitory mechanisms effect tumour growth. In particular, we are interested in explaining the shrinkage/regrowth phenomena observed by Folkman and Hochberg [24]. What properties should an inhibitor possess to yield such qualitative behaviour? The paucity of experimental information available in the literature means that little is known about how inhibitors operate. For example, does an inhibitor function by destroying the nutrient value of some species or does it reduce the cell proliferation rate by modifying the cell DNA structure? Further, are there qualitative differences between these modes of operation? In an attempt to answer these questions, the following inhibitory mechanisms are now postulated.

- Inhibitor Free ($\beta \equiv 0$): $g_1 = 0 = g_2, \bar{S} = s(\sigma - \tilde{\sigma})$.
- Inhibitor affects cell proliferation rate, not nutrient concentration; $g_1 = 0, g_2 = \gamma_2\beta$, $\bar{S} = s(\sigma - \tilde{\sigma})(1 - \beta/\tilde{\beta})$.
- Inhibitor affects nutrient species, not cell proliferation rate; $g_1 = \gamma_1\beta, g_2 = \gamma_2\beta$, $\bar{S} = s(\sigma - \tilde{\sigma})$.
- Inhibitor affects both nutrient concentration and cell proliferation rate; $g_1 = \gamma_1\beta, g_2 = \gamma_2\beta, \bar{S} = s(\sigma - \tilde{\sigma})(1 - \beta/\tilde{\beta})$.

We remark here that, to simplify the analysis, the interaction terms $g_1(\sigma, \beta), g_2(\sigma, \beta)$ depend only on the inhibitor concentration, β, in a simple, linear fashion. Thus equation (2.2) decouples from the system, with β entering the reduced model as a prescribed forcing term in (2.1) and/or a renormalisation of the proliferation rate in (2.3). Whilst other expressions for g_1, g_2 which couple the two reaction-diffusion equations are probably more realistic, they are not considered here since they are not amenable to simple analysis.

Nondimensionalisation

Before continuing with our analysis, we express the moving boundary problem in dimensionless form. Time is rescaled with the growth time of the tumour T say whilst distance is scaled with a typical tumour radius, $R(t = 0) = R_0$ say. Thus, we introduce the dimensionless variables $(\bar{r}, \bar{t}) = (r/R_0, t/T)$, and rescale the dependent variables and key parameters as follows:

$$\bar{\sigma}(\bar{r},\bar{t}) = \sigma(r,t)/\Sigma,\ \bar{\beta}(\bar{r},\bar{t}) = \beta(r,t)/B,\ \bar{R}(\bar{t}) = R(t)/R_0,\ \bar{r}_{in}(\bar{t}) = r_{in}(t)/R_0, \tag{2.10}$$

$$(\bar{\sigma}_\infty, \bar{\sigma}_{nec}, \bar{\tilde{\sigma}}) = \Sigma^{-1}(\sigma_\infty, \sigma_{nec}, \tilde{\sigma}),\ (\bar{\beta}_\infty, \bar{\tilde{\beta}}) = B^{-1}(\beta_\infty, \tilde{\beta}), \tag{2.11}$$

$$\bar{\Gamma} = \Gamma R_0^2/D_1,\ \bar{\lambda} = \lambda/s, \tag{2.12}$$

$$\bar{\gamma}_1 = \gamma_1 R_0^2 B/D_1\Sigma,\ \bar{\gamma}_2 = \gamma_2 R_0^2/D_2,\ \bar{s} = sT, \tag{2.13}$$

where (Σ, B) are typical nutrient and inhibitor concentrations. Dropping the bars, equations (2.1)-(2.3) transform to give:

$$0 = \frac{1}{r^2}\frac{\partial}{\partial r}\left(r^2\frac{\partial \sigma}{\partial r}\right) - [\Gamma\sigma + \gamma_1\beta]H(r - r_{in}), \tag{2.14}$$

$$0 = \frac{1}{r^2}\frac{\partial}{\partial r}\left(r^2\frac{\partial \beta}{\partial r}\right) - \gamma_2\beta H(r - r_{in}), \tag{2.15}$$

$$\frac{dR}{dt} = \frac{s}{R^2}\left\{\int_{r_{in}}^{R}(\sigma - \tilde{\sigma})(1 - \beta/\tilde{\beta})r^2 dr - \lambda r_{in}^3\right\}, \tag{2.16}$$

subject to

$$\frac{\partial \sigma}{\partial r} = 0 = \frac{\partial \beta}{\partial r} \quad \text{on} \quad r = 0, \tag{2.17}$$

$$\sigma = \sigma_\infty,\quad \beta = \beta_\infty,\quad \text{on} \quad r = R(t), \tag{2.18}$$

$$\sigma, \frac{\partial \sigma}{\partial r}, \beta, \frac{\partial \beta}{\partial r} \quad \text{continuous across} \quad r = r_{in}(r), \tag{2.19}$$

$$\sigma = \sigma_{nec} \quad \text{on} \quad r = r_{in}(r), \tag{2.20}$$

$$R(0) = 1. \tag{2.21}$$

The proliferation rate (2.4) has been used in equation (2.16).

3. Numerical Simulations

Numerical solution of the mathematical model defined by equations (2.14)-(2.21) necessitates following the two free boundaries $R(t)$ and $r_{in}(t)$. Since $R(t)$ satisfies an integro-differential equation, tracking the outer tumour radius is relatively straightforward. By contrast, the necrotic core radius is defined implicitly by (2.19) and evolves on different timescales, depending on the tumour's size. For example, the asymptotic analysis of section 5 demonstrates how immediately after the onset of necrosis r_{in} evolves on a rapid timescale during which R remains approximately constant. For these reasons, in this paper we restrict attention to simple nutrient/inhibitor consumption terms for which solution of the mathematical model can be viewed as a two-stage process. First, solution of the governing reaction-diffusion equations yields σ, β in terms of the tumour radii $R(t)$ and $r_{in}(t)$. Secondly, expressions governing R and r_{in} are obtained by imposing equation (2.20) and substituting with σ and β in (2.16).

3.1 Inhibitor-Free Solutions

With $\beta \equiv 0$, and $S(\sigma, \beta) = s(\sigma - \tilde{\sigma})$, solution of equation (2.14), subject to (2.17)–(2.19), yields the following expression for the nutrient concentration, σ:

$$\sigma = \begin{cases} \sqrt{\Gamma} A, & \text{for } \rho \in (0, r_{in}), \\ \dfrac{A}{r}\left(\sinh\sqrt{\Gamma}(r - r_{in}) + \sqrt{\Gamma} r_{in} \cosh\sqrt{\Gamma}(r - r_{in})\right), & \text{for } \rho \in (r_{in}, 1), \end{cases} \tag{3.1}$$

where

$$A = \sigma_\infty R / (\sinh\sqrt{\Gamma}(R - r_{in}) + \sqrt{\Gamma} r_{in} \cosh\sqrt{\Gamma}(R - r_{in})).$$

Imposing (2.20) we deduce that $\sqrt{\Gamma} A = \sigma_{nec}$ and, hence, that r_{in} is related to R by the following equation:

$$\left(\frac{\sigma_\infty}{\sigma_{nec}}\right)\sqrt{\Gamma} R = \sinh\sqrt{\Gamma}(R - r_{in}) + \sqrt{\Gamma} r_{in} \cosh\sqrt{\Gamma}(R - r_{in}). \tag{3.2}$$

Substituting with σ in (2.16), and noting that $A = \sigma_{nec}/\sqrt{\Gamma}$, we obtain the following differential equation for $R(t)$:

$$\begin{aligned} R^2 \frac{dR}{dt} = \frac{s\sigma_{nec}}{\Gamma^{3/2}} & \left\{\sqrt{\Gamma}(R - r_{in}) \cosh\sqrt{\Gamma}(R - r_{in}) + (\Gamma R r_{in} - 1)\sinh\sqrt{\Gamma}(R - r_{in})\right\} \\ & - s\left(\frac{\tilde{\sigma}}{3}(R^3 - r_{in}^3) + \lambda r_{in}^3\right). \end{aligned} \tag{3.3}$$

The coupled equations (3.2) and (3.3) can be solved simultaneously, subject to $R(0) = 1$, to determine $R(t)$ and $r_{in}(t)$. However, in order to simplify the following analysis, it is convenient to introduce the scaled radii

$$\eta(t) = \sqrt{\Gamma} R(t) \text{ and } \zeta(t) = \sqrt{\Gamma} r_{in}(t),$$

so that equations (3.2) and (3.3) transform to give

$$\left(\frac{\sigma_\infty}{\sigma_{nec}}\right)\eta = \sinh(\eta-\zeta) + \zeta\cosh(\eta-\zeta), \tag{3.4}$$

$$\eta^2\frac{d\eta}{dt} = s\sigma_{nec}\left\{(\eta-\zeta)\cosh(\eta-\zeta) + (\eta\zeta-1)\sinh(\eta-\zeta)\right\} - s\left(\frac{\tilde{\sigma}}{3}(\eta^3-\zeta^3)+\lambda\zeta^3\right), \tag{3.5}$$

with $\eta(0) = \sqrt{\Gamma}$.

Before presenting numerical results, we mention how (3.4) and (3.5) are modified for non-necrotic tumours. Referring to [16], we remark that if $\zeta = 0$ then σ_{nec} should be replaced by $\sigma(0)$. In this case, equation (3.4) defines $\sigma(0) = \sigma_\infty\eta/\sinh\eta$ and (3.5) becomes

$$\eta^2\frac{d\eta}{dt} = s\sigma_\infty\eta\left(\frac{\eta}{\tanh\eta}-1\right) - \frac{s\tilde{\sigma}\eta^3}{3}.$$

Figures 1(a)-(c) summarise the range of qualitative behaviour obtained when the linear, inhibitor-free proliferation rate is employed. Three possible outcomes are observed. In the first case, both η and ζ increase, or decrease, monotonically towards equilibrium values η_∞ and ζ_∞, say, which are independent of $\eta(0)$ and $\zeta(0)$. In the second case, all initial data evolve monotonically to a non-necrotic tumour configuration for which $\eta_\infty > \zeta_\infty = 0$. In the third case, η and ζ decay monotonically to zero, so that the tumour eventually disappears. Typical examples of each mode of behaviour are reproduced in figures 1(a)-(c). From the simulations we observe that the type of behaviour which is realised is strongly related to the size of $\tilde{\sigma}$ relative to σ_∞ and σ_{nec}: as $\tilde{\sigma}$ decreases, decay of the tumour to zero is superceded first by evolution of the tumour to a steady, non-necrotic configuration for moderate values of $\tilde{\sigma}$ and to a steady necrotic configuration for even smaller values of $\tilde{\sigma}$. (The discussion in section 4 of the existence of steady-state tumour configurations renders this result more explicit.)

The effect that the choice of the proliferation rate has on the tumour's growth characteristics becomes apparent when the linear proliferation rate (2.4) is replaced by a logistic term and we fix

$$S(\sigma,\beta) = s\sigma\left(1-\frac{\sigma}{\hat{\sigma}}\right)$$

in (2.16). This modification leaves equation (3.4), relating ζ to η, unchanged whereas (3.5) is superceded by the following ordinary differential equation for η:

$$\begin{aligned}\eta^2\frac{d\eta}{dt} &= s\sigma_{nec}\left\{(\eta-\zeta)\cosh(\eta-\zeta) + (\eta\zeta-1)\sinh(\eta-\zeta)\right\} - s\lambda\zeta^3 \\ &\quad - \frac{s\sigma_{nec}^2}{2\hat{\sigma}}\left(\frac{(1+\zeta^2)}{2}\sinh 2(\eta-\zeta) + \zeta\cosh 2(\eta-\zeta) + (\zeta^2-1)\eta - \zeta^3\right).\end{aligned} \tag{3.6}$$

Numerical simulations suggest that, in this case, only two possible outcomes occur: either the tumour decays to zero or it attains a steady, necrotic configuration. The type of behaviour which is realised depends on the size of $\hat{\sigma}$ relative to σ_∞ and σ_{nec}. For example, for small values of $\hat{\sigma}$ all tumour configurations decay to zero whereas for large values of $\hat{\sigma}$ all tumours evolve to a necrotic configuration. The behaviour for intermediate values of $\hat{\sigma}$ depends on the initial tumour size: small tumours decay to zero whereas larger tumours evolve to a necrotic configuration (figure 2). These results, together with figures 1(a)-(c), demonstrate how important accurate knowledge of the proliferation rate is when assessing the growth characteristics of a tumour.

3.2 Inhibitor-Present Solutions

For the general case, in which the inhibitor acts both by reducing the nutrient levels inside the tumour and by reducing the cell proliferation rate, equations (2.14)-(2.15) may be integrated, subject to (2.17)–(2.19) to obtain the following expressions for σ, β:

$$\sigma = \begin{cases} \sigma_{nec}, & \text{for } r \in (0, r_{in}), \\ \dfrac{A_\sigma}{r}(\sinh\sqrt{\Gamma}(r - r_{in}) + \sqrt{\Gamma} r_{in} \cosh\sqrt{\Gamma}(r - r_{in})) + \Delta\beta, & \text{for } r \in (r_{in}, R), \end{cases} \tag{3.7}$$

and

$$\beta = \begin{cases} \beta_{nec}, & \text{for } r \in (0, r_{in}), \\ \dfrac{A_\beta}{r}(\sinh\sqrt{\gamma_2}(r - r_{in}) + \sqrt{\gamma_2} r_{in} \cosh\sqrt{\gamma_2}(r - r_{in})), & \text{for } r \in (r_{in}, R), \end{cases} \tag{3.8}$$

where

$$A_\sigma = (\sigma_\infty - \Delta\beta_\infty)R/(\sinh\sqrt{\Gamma}(R - r_{in}) + \sqrt{\Gamma} r_{in} \cosh\sqrt{\Gamma}(R - r_{in})), \tag{3.9}$$

$$A_\beta = \beta_\infty R/(\sinh\sqrt{\gamma_2}(R - r_{in}) + \sqrt{\gamma_2} r_{in} \cosh\sqrt{\gamma_2}(R - r_{in})), \tag{3.10}$$

$$\Delta = \gamma_1/(\gamma_2 - \Gamma), \tag{3.11}$$

and β_{nec} is defined in terms of the scaled variables $\eta = \sqrt{\Gamma}R$ and $\zeta = \sqrt{\Gamma} r_{in}$ as follows:

$$\beta_{nec} = \beta_\infty \theta\eta/(\sinh\theta(\eta - \zeta) + \theta\zeta \cosh\theta(\eta - \zeta)). \tag{3.12}$$

In (3.12), we have introduced $\theta = \sqrt{\gamma_2/\Gamma}$. Imposing (2.20) yields the following expression which defines $\zeta = \sqrt{\Gamma} r_{in}$ in terms of $\eta = \sqrt{\Gamma}R$ and which generalises (3.4) to the case $\beta > 0$:

$$\left(\frac{\sigma_\infty - \Delta\beta_\infty}{\sigma_{nec} - \Delta\beta_{nec}}\right)\eta = \sinh(\eta - \zeta) + \zeta\cosh(\eta - \zeta). \tag{3.13}$$

Substituting with σ and β from (3.7) and (3.8) in (2.16) it is possible to derive an equation for η, which generalises (3.5) to the case $\beta > 0$. Rather than presenting this cumbersome expression, for clarity we simply rewrite (2.16) in terms of the scaled variables η and ζ:

$$\eta^2\frac{d\eta}{dt} = s\left\{\int_\zeta^\eta (\sigma(\rho/\sqrt{\Gamma},t) - \tilde{\sigma})\left(1 - \frac{\beta(\rho/\sqrt{\Gamma},t)}{\tilde{\beta}}\right)\rho^2 d\rho - \lambda\zeta^3\right\}. \tag{3.14}$$

As mentioned above, our model incorporates two mechanisms for inhibitor action: either as a sink of nutrient in (2.14) (indirect action) or by reducing the cell proliferation rate in (2.16) (direct action). For comparison with the inhibitor-free results presented in section 3.1, we examine the effect that these modes of action, taken separately and together, have on the tumour's development. Tables 1 to 3 below summarise these results, showing how η_∞ and ζ_∞ vary with the mode of inhibitor action.

With $\tilde{\sigma} = 0.2 < \sigma_{nec}$, table 1 shows that both the direct and indirect modes of inhibitor action have the capacity to reduce the size of the equilibrium tumour. Indeed, in this case, presence of the inhibitor has a beneficial effect in all cases. With the inhibitor acting in both manners ($\gamma_1 = 0.8, \tilde{\beta} = 0.5$), a change in the qualitative behaviour of the system occurs, with the appearance of two equilibrium states ($\eta_\infty = 2.38, 0.00$). From figure 3 we observe that in this case if, prior to the inhibitor's introduction, the tumour is sufficiently small (here $\eta(0) < 0.98$) then the tumour disappears. For larger values of $\eta(0)$, as before, the tumour evolves to a finite size.

Table 1 ($\tilde{\sigma} = 0.2$)

	γ_1	$\tilde{\beta}$	η_∞	ζ_∞
	0.0	$+\infty$	7.40	6.00
	0.01	5.0	6.82	5.42
	0.80	5.0	4.77	3.77
	0.01	0.9	4.10, 0.00	2.62, 0.00
(Fig 3)	0.80	0.9	2.38, 0.00	1.29, 0.00
	0.01	0.5	0.00	0.00
	0.80	0.5	0.00	0.00

Referring now to table 2, with $\sigma_{nec} < \tilde{\sigma} = 0.7 < \sigma_\infty$, we note that in most cases presence of the inhibitor has a beneficial effect, reducing η_∞. However, direct action of the inhibitor ($\gamma_1 = 0.8, \tilde{\beta} = 0.5$) actually increases the equilibrium size of the tumour. Thus, in this case presence of the inhibitor does not always improve the situation.

Table 2 ($\tilde{\sigma} = 0.7$)

γ_1	$\tilde{\beta}$	η_∞	ζ_∞
0.00	$+\infty$	1.51	0.00
0.01	5.0	1.48	0.00
0.80	5.0	1.06	0.00
0.01	0.9	0.00	0.00
0.80	0.9	0.00	0.00
0.01	0.5	0.00	0.00
0.80	0.5	1.90, 0.00	0.71, 0.00

The results presented in table 3, with $\sigma_\infty < \tilde{\sigma} = 0.9$, demonstrate how treatment with an inhibitor can sometimes exacerbate the situation. In this case direct action of the inhibitor introduces a stable, nontrivial tumour whose size and structure depends on the strength of the inhibitor action. However, the necrotic tumour is only obtained when $\eta(0) > 1.20$: if $\eta(0) < 1.20$ then the tumour decays to zero.

Table 3 ($\tilde{\sigma} = 0.9$)

γ_1	$\tilde{\beta}$	η_∞	ζ_∞
0.00	$+\infty$	0.00	0.00
0.01	5.0	0.00	0.00
0.80	5.0	0.00	0.00
0.01	0.9	0.88	0.00
0.80	0.9	0.86	0.00
0.01	0.5	2.72	1.06
0.80	0.5	2.86	1.80

4. Steady-State Analysis

The numerical results of the previous section indicate that both the parameter values and the functional forms employed in the model can affect a tumour's potential for growth. For example, for the inhibitor-free model, the existence of a nontrivial steady solution having a necrotic core is predicted in figure 1(a) whereas in figure 1(c), for a different set of parameter values, the tumour disappears. In this section, by seeking time-independent solutions of equations (2.14)-(2.21), we investigate how the existence and multiplicity of steady solutions is affected by the choice of the proliferation rate and the associated parameter values. The stability of these solutions is then discussed in section 5.

4.1 Inhibitor-Free Steady Solutions

With $d/dt = 0$ equations (3.4)-(3.5) define the steady-state scaled tumour radii η and ζ:

$$(\eta-\zeta)\cosh(\eta-\zeta) + (\eta\zeta-1)\sinh(\eta-\zeta) = \left(\frac{\tilde{\sigma}}{3\sigma_{nec}}\right)(\eta^3-\zeta^3) + \left(\frac{\lambda}{\sigma_{nec}}\right)\zeta^3,$$

$$\sinh(\eta-\zeta) + \zeta\cosh(\eta-\zeta) = \left(\frac{\sigma_\infty}{\sigma_{nec}}\right)\eta.$$

For the case $\zeta = 0$ the above equations reduce to give the following expression for η [16]:

$$\tanh\eta = \frac{\eta}{1+\tilde{\sigma}\eta^2/3\sigma_\infty}.$$

Figure 4 illustrates the variation of η and ζ with $\tilde{\sigma}$, holding $\sigma_\infty, \sigma_{nec}$ and λ fixed. From this diagram we note that, whilst the trivial solution $\eta = \zeta = 0$ persists for all parameter values, nontrivial solutions exist only when $\tilde{\sigma} < \sigma_\infty$. Indeed, by focussing on a neighbourhood of $\tilde{\sigma} = \sigma_\infty$ it is possible to show that a branch of non-necrotic solutions are created as $\tilde{\sigma}$ decreases through σ_∞. We remark also that where they exist the nontrivial solutions are unique.

Increasing λ clearly has no effect on non-necrotic tumours. In particular, changes in λ leave the points **A** and **B** on figure 4 fixed. However, by focusing on the limit $\tilde{\sigma} \sim \delta\bar{\tilde{\sigma}}$ $(0 < \delta \ll 1)$ we gain some insight into how the points $\mathbf{C}_\eta$ and $\mathbf{C}_\zeta$ depend on λ. For example, if $\lambda \sim \bar{\lambda}/\delta^3$ then the leading order steady-state solutions can be written in the form $\eta \sim \bar{\eta}$ and $\zeta \sim \delta\bar{\zeta}$ where

$$\frac{\sinh\bar{\eta}}{\bar{\eta}} = \frac{\sigma_\infty}{\sigma_{nec}} \text{ and } \bar{\zeta}^3 = \frac{\sigma_{nec}}{\bar{\lambda}}(\bar{\eta}\cosh\bar{\eta} - \sinh\bar{\eta}).$$

By continuity, we deduce that increasing λ reduces both $\mathbf{C}_\eta$ and $\mathbf{C}_\zeta$. Focussing now on σ_{nec}, it is possible to show that increasing σ_{nec} leaves the point **A** fixed, moves **B** closer to **A**, and reduces both $\mathbf{C}_\eta$ and $\mathbf{C}_\zeta$.

4.2 Inhibitor-Present Steady Solutions

With $d/dt = 0$, equations (3.12)-(3.14) define the steady-state radii η and ζ when $\beta > 0$. Figures 5 (a,b,c) portray the variation of η and ζ with $\tilde{\sigma}$ for the three choices of $\tilde{\beta}$ considered in tables 1 to 3 of section 3.2. The figures not only summarise the different types of behaviour that the inhibitor may induce in a tumour but also provide some indication of its success in fighting the tumour. For example, comparing figures 4 and 5(a), we note that, in this case, presence of the inhibitor simply reduces the inhibitor-free steady-state configuration where it exists. By contrast, the appearance of non-unique solutions in figure 5(b) marks a qualitative change in the action of the inhibitor. However, provided that $\tilde{\sigma} < \sigma_\infty$ the resulting steady-states are smaller and possibly zero in the presence of the inhibitor. On the basis of the results presented in tables 1 to 3 and the numerical simulations depicted in figure 3, it seems reasonable to assume that the lower branch of nontrivial solutions is unstable and separates the stable necrotic configuration from a stable, tumour-free configuration. The appearance of nontrivial solutions for $\tilde{\sigma} > \sigma_\infty$ is also new. In this case the inhibitor acts detrimentally, destabilising the trivial solutions and enabling the system to support a tumour where the inhibitor-free system did not. Turning finally to figure 5(c), we note that, in this case, provided that $\tilde{\sigma} < \sigma_\infty$ the inhibitor eliminates the tumour whereas for $\tilde{\sigma} > \sigma_\infty$, as in figure 5(b), presence of the inhibitor leads to the appearance of a tumour.

5. Asymptotic Analysis

In section 3 expressions governing the evolution of the scaled tumour radii η and ζ were derived for different proliferation rates, and in the presence or absence of an inhibitor β. Taken with the steady state analysis presented in section 4, these results provide some insight into the local stability of the different tumour configurations. For example, referring to figure 4, with $\beta = 0$, we anticipate that, where it exists, the nontrivial steady state is stable. By contrast, referring now to figure 5(b), with $\beta > 0$, we anticipate that the upper solution on each of the two branches is stable, the lower branch unstable, and the trivial solution stable where an even number of nontrivial solutions exist.

In practice it is possible to establish local stability properties of the steady solutions by examining the evolution of small perturbations about the steady states. However, due to the complexity of the governing equations such an approach is not particularly instructive here. Rather, we focus on the evolution of the tumour in two limiting cases which are of practical interest: immediately after the onset of necrosis ($0 < \zeta \ll 1$) and when the width of the proliferating rim is small ($0 < \eta - \zeta \ll 1$). (The case $0 < \eta \ll 1$ is not considered here since it is discussed in detail in [16]. There the appearance of a nontrivial non-necrotic solution as $\tilde{\sigma}$ decreases through σ_∞ is shown to coincide with the loss of stability of the trivial steady state.) The asymptotic analysis enables us to investigate the effect that the different proliferation rates and modes of inhibitor action have on the tumour's growth for the cases of interest. It is anticipated that the resulting approximate expressions for

η and ζ (or, $R(t)$ and $r_{in}(t)$) which result could be used to estimate key parameters from *in vitro* data on multicellular spheroids [24].

5.1 Inhibitor-Free Analysis

Before presenting the asymptotic analysis we first explain why the existence of nontrivial solutions is restricted to $\tilde{\sigma} < \sigma_\infty$. Substituting with (2.4) in (2.16) and fixing $\beta = 0$ leads to the following equation for dR/dt:

$$R^2 \frac{dR}{dt} = s \int_{r_{in}}^{R} (\sigma - \tilde{\sigma}) r^2 dr - \lambda r_{in}^3, \tag{5.1}$$

where σ satisfies (2.14) and (2.17)-(2.20). By the maximum principle [25], σ attains its maximum value on the tumour boundary where $\sigma(R,t) = \sigma_\infty$. Thus if $\tilde{\sigma} > \sigma_\infty$ then the integrand in (5.1) is negative and, hence, $dR/dt < 0 \ \forall \ r_{in} \in [0, R)$. In particular, for $\tilde{\sigma} > \sigma_\infty$ no nontrivial solutions exist and the trivial, tumour-free state is stable.

Small necrotic core analysis. Assuming that the necrotic core is initially $O(\epsilon)$ ($0 < \epsilon \ll 1$), we seek solutions to (3.4)-(3.5) in the form

$$\eta \sim \eta_0 + \epsilon \eta_1 + \epsilon^2 \eta_2 \text{ and } \zeta \sim \epsilon \zeta_1, \tag{5.2}$$

the small parameter ϵ chosen so that $\zeta_1(t = 0) = 1$. Substituting with (5.2) in (3.4), and equating to zero $O(1)$-terms, we deduce that η_0 satisfies:

$$\frac{\sigma_\infty}{\sigma_{nec}} = \frac{\sinh \eta_0}{\eta_0}. \tag{5.3}$$

Thus, provided that $\sigma_\infty > \sigma_{nec}$, there exists a nontrivial solution η_0 which is independent of time. Continuing with our expansion we deduce from (3.4) that $\eta_1 = 0$ and ζ_1 is related to η_2 in the following way:

$$\zeta_1^2 = \frac{2(\cosh \eta_0 - \sigma_\infty / \sigma_{nec})}{\sinh \eta_0} \eta_2. \tag{5.4}$$

We remark that, since $\zeta_1(0) = 1$, equation (5.4) automatically defines $\eta_2(0)$.

With η_0 and η_1 independent of time, substituting with (5.2) in equation (3.5) yields a differential equation which is singular in the limit as $\epsilon \to 0$. In order to regularise the problem we introduce the transient timescale $\tau = t/\epsilon^2$ and rescale (3.5) accordingly. Now, equating to zero $O(1)$-terms we recover the following equation for $\eta_2(\tau)$:

$$\frac{d\eta_2}{d\tau} = \frac{s\sigma_{nec}}{\eta_0^2}\left\{\eta_0 \cosh\eta_0 - \sinh\eta_0 - \frac{\tilde{\sigma}}{\sigma_{nec}}\frac{\eta_0}{3}\right\} \equiv \Lambda, \text{ say.} \tag{5.5}$$

Reverting to the original timescale $t = \epsilon^2\tau$, we deduce that η and ζ are given by

$$\eta \sim \eta_0 + \epsilon^2\eta_2(0) + \Lambda t, \tag{5.6}$$

$$\zeta \sim \left(\epsilon^2 + \frac{\eta_0\cosh\eta_0 - \sinh\eta_0}{\eta_0\sinh\eta_0}2\Lambda t\right)^{1/2}, \tag{5.7}$$

with η_0 and $\eta_2(0)$ defined in terms of $\sigma_\infty/\sigma_{nec}$ by (5.3) and (5.4), and growth of the tumour is predicted when $\Lambda > 0$. From the definition of Λ, we infer that growth results if

$$\frac{\tilde{\sigma}}{\sigma_{nec}} < \frac{3(\eta_0\cosh\eta_0 - \sinh\eta_0)}{\eta_0},$$

and the expansion (5.6)-(5.7) remains valid until $t \sim O(1)$, by which time the necrotic core is $O(1)$. Otherwise, if $\Lambda < 0$, shrinkage of the tumour is predicted and the necrotic core disappears in finite time t_D where, from (5.7),

$$t_D = \frac{\epsilon^2\eta_0\sinh\eta_0}{2\,|\Lambda|\,(\eta_0\cosh\eta_0 - \sinh\eta_0)}.$$

The case $\Lambda = 0$, which occurs only for particular values of the parameters $\tilde{\sigma}/\sigma_{nec}$ and $\sigma_\infty/\sigma_{nec}$, gives rise to a steady, necrotic configuration. By considering higher order terms in the power series expansion (5.2) it is possible to shows that this solution is indeed stable with respect to small perturbations.

The above results indicate that it is the balance between the parameter groupings $\tilde{\sigma}/\sigma_\infty \in (0,1)$ and $\sigma_{nec}/\sigma_\infty \in (0,1)$ which governs the sign of Λ and, hence, the viability of the necrotic core. We note that if $\tilde{\sigma} < \sigma_{nec}$ then $\Lambda > 0$ and persistence of the necrotic core is predicted. This result can also be derived from (5.1), using an argument similar to that used to prove stability of the trivial solution when $\tilde{\sigma} > \sigma_\infty$. In this case, if $\tilde{\sigma} < \sigma_{nec}$ then the integrand in (5.1) is positive $\forall\, r \in (r_{in}, R)$ so that, if a nontrivial steady solution occurs, it must possess a necrotic core.

Thin proliferating rim analysis. Assuming, now, that the width of the proliferating region is $O(\delta)$ $(0 < \delta \ll 1)$, we seek solutions to (3.4)-(3.5) in the form:

$$\eta \sim \eta_0 + \delta\eta_1 + \delta^2\eta_2 \quad \text{and} \quad \zeta \sim \eta_0 + \delta\zeta_1 + \delta^2\zeta_2. \tag{5.8}$$

In addition, we assume a regular expansion for $\sigma_\infty \sim \sigma_{\infty 0} + \delta\sigma_{\infty 1} + \delta^2\sigma_{\infty 2}$. The reason for considering an expansion for σ_∞ becomes clear when we substitute with (5.8) in (3.4). Equating to zero coefficients of $O(\delta^n)$ yields the following relations:

$$\begin{aligned} O(1): &\quad \sigma_{\infty 0} = \sigma_{nec}, \\ O(\delta): &\quad \sigma_{\infty 1} = 0, \\ O(\delta^2): &\quad (\eta_1 - \zeta_1)^2 = 2\sigma_{\infty 2}/\sigma_{nec}. \end{aligned}$$

Thus, we deduce that $\sigma_{\infty 0} = \sigma_{nec}$ is a necessary condition for the existence of a thin proliferating rim . The $O(\delta^2)$ relation shows that, in this limit, the width of the proliferating rim is directly related to the difference between the external and the necrotic nutrient concentrations, σ_∞ and σ_{nec} respectively. Indeed the dependence of $(\eta - \zeta)$ on σ_∞ and σ_{nec} agrees with the expression assumed by Greenspan [4].

Substituting with (5.8) in (3.5), and using the expressions derived from (3.4), we obtain the following equations for η_i $(i = 0, 1, ...)$:

$$\begin{aligned} O(1): &\quad \frac{d\eta_0}{dt} = -s\lambda\eta_0, \\ O(\delta): &\quad \frac{d\eta_1}{dt} = s\sigma_{nec}\left(1 - \frac{\tilde{\sigma}}{\sigma_{nec}} + \frac{3\lambda}{\sigma_{nec}}\right)\left(\frac{2\sigma_{\infty 2}}{\sigma_{nec}}\right)^{1/2} - s\lambda\eta_1 \equiv s(\phi - \lambda\eta_1), \text{ say.} \end{aligned}$$

Integrating with respect to time, we deduce that

$$\begin{aligned} \eta &\sim \eta_0(0)e^{-s\lambda t} + \frac{\delta\phi}{\lambda}(1 - e^{-s\lambda t}), \\ \eta - \zeta &\sim \delta\left(\frac{2\sigma_{\infty 2}}{\sigma_{nec}}\right)^{1/2} = \left(\frac{2(\sigma_\infty - \sigma_{nec})}{\sigma_{nec}}\right)^{1/2}, \\ \sigma_\infty &\sim \sigma_{nec} + \delta^2\sigma_{\infty 2} > \sigma_{nec}. \end{aligned}$$

Thus, if $\lambda \sim O(1)$ then shrinkage of both η and ζ is predicted, with the rate of necrosis λ dominating the regression. This contrasts with the small necrotic core analysis presented above. There the rate of apoptosis $\tilde{\sigma}$ dominated the growth or shrinkage of the necrotic core, and the effect of apoptosis was only evident as a higher order effect.

Reducing the rate of necrosis, so that $\lambda = \delta\bar{\lambda}$, does not affect the expressions for $\eta - \zeta$ and σ_∞. However, the expression for η is modified to give:

$$\eta \sim \eta_0(0) + \delta s \sigma_{nec} \left\{ \left(1 - \frac{\tilde{\sigma}}{\sigma_{nec}}\right) \left(\frac{2\sigma_{\infty 2}}{\sigma_{nec}}\right)^{1/2} - \frac{\bar{\lambda}\eta_0(0)}{\sigma_{nec}} \right\} t. \tag{5.9}$$

As when $\lambda \sim O(1)$, if $\tilde{\sigma} > \sigma_{nec}$ then tumour regression is predicted for all values of $\eta_0(0)$. By contrast, if $\tilde{\sigma} < \sigma_{nec}$ then η evolves monotonically to an equilibrium value η^* which is given by:

$$\eta^* = \frac{\sigma_{nec}}{\bar{\lambda}} \left(1 - \frac{\tilde{\sigma}}{\sigma_{nec}}\right) \left(\frac{2\sigma_{\infty 2}}{\sigma_{nec}}\right)^{1/2}.$$

By considering values of $\eta_0(0)$ which are larger and smaller than η^* it is clear that η^* defines a stable necrotic tumour configuration which is attained in the limit $\sigma_\infty \to \sigma_{nec}$ and has a proliferating rim of width $O((\sigma_\infty - \sigma_{nec})^{1/2})$ [4].

In summary, we deduce that when the necrotic core is small ($0 < \zeta \sim \epsilon\zeta_1(t) \ll 1$) changes in the necrotic radius occur on a much larger scale than changes in the outer tumour radius ($\eta(t) - \eta(0) \sim O(\epsilon^2)$). In particular, referring to equations (5.6)-(5.7), the speed of the necrotic radius is more rapid than that of the outer tumour radius: $d\zeta/dt \sim t^{-1/2}$ whereas $d\eta/dt \sim$ constant. The balance between the rate of apoptosis and the nutrient concentration at which necrosis is initiated determines whether growth or shrinkage of the necrotic core results: the rate of cell degradation due to necrosis does not affect the results. In particular, if $\sigma_{nec} > \tilde{\sigma}$ then the necrotic core persists. By contrast, for the thin proliferating rim analysis λ is the dominant cell loss mechanism. If $\lambda \sim O(1)$ then regression of the tumour occurs. Reducing the rate of apoptosis, so that $\lambda = \delta\bar{\lambda}$ ($0 < \delta \ll 1$), a stable necrotic steady state is predicted if $\tilde{\sigma} < \sigma_{nec}$. A necessary condition for the existence of solutions having thin proliferating rim is that $0 < \sigma_\infty - \sigma_{nec} \sim O(\delta^2)$, this difference defining the width of the proliferating rim.

It is anticipated that the asymptotic analysis presented above could be used to estimate parameters from experimental data describing the evolution of the necrotic and outer tumour radii. In particular, by contrasting the small necrotic core and the thin proliferating rim limits it should be possible to assess the relative importance of the two cell loss mechanisms, apoptosis and necrosis.

5.2 Inhibitor-Present Analysis

It is possible to extend the analysis of section 5.1 to the case for which $\beta > 0$. For example, by considering the following, inhibitor-present analogue of (5.1)

$$R^2 \frac{dR}{dt} = s \int_{r_{in}}^{R} (\sigma - \tilde{\sigma})(1 - \beta/\tilde{\beta}) r^2 dr - \lambda r_{in}^3,$$

it is easy to see that if $\tilde{\beta} > \beta_\infty$ then the trivial solution is both stable and unique whenever $\tilde{\sigma} > \sigma_\infty$ (see figure 5(a)). Similarly, if $\tilde{\sigma} < \sigma_{nec}$ and $\tilde{\beta} < \beta_{nec} = \beta(r_{in}, t)$ then the trivial solution is again unique and stable (see figure 5(c)).

We now consider how the presence of an inhibitor affects the growth of tumours which have small necrotic cores. To do this, we seek solutions to (3.12)–(3.14) of the form

$$\eta \sim \eta_0 + \epsilon^2 \eta_2, \quad \zeta \sim \epsilon \zeta_1, \quad \beta_{nec} \sim \beta_{n0} + \epsilon^2 \beta_{n2},$$

The same qualitative behaviour observed when $\beta = 0$ is recovered (see figure 3). Thus there is a rapid timescale $t \sim O(\epsilon^2)$ during which the outer tumour radius remains constant to $O(\epsilon^2)$ whilst the necrotic core grows (or shrinks, depending on the parameter values) rapidly. Unfortunately, the detailed analysis is much less tractable than for the case $\beta = 0$. For example, using (3.12) and (3.13), and introducing $\theta = \sqrt{\gamma_2/\Gamma}$, it is possible to show that (5.3) is superceded by the following expression defining η_0 in terms of the key parameters:

$$\frac{\sigma_\infty}{\sigma_{nec}} = \frac{\sinh \eta_0}{\eta_0} + \frac{\Delta \beta_\infty}{\sigma_{nec}} \left(1 - \frac{\theta \eta_0}{\sinh \eta_0} \right).$$

Since the corresponding equations for η_2 and ζ_1 are rather cumbersome, for simplicity any further discussion of the small necrotic core analysis is omitted.

In contrast to the small necrotic core analysis mentioned above, that for the asymptotic limit $0 < \eta - \zeta \ll 1$ generalises naturally to the case $\beta > 0$. In particular, with $\lambda \sim O(1)$, we obtain the following, modified expressions for η and ζ from (3.12)-(3.14):

$$\eta = \eta_0(0) e^{-s\lambda t} + \frac{\delta \bar{\phi}}{\lambda} (1 - e^{-s\lambda t}),$$

$$\eta - \zeta \sim \delta(\eta_1 - \zeta_1) = \delta \left(\frac{2\sigma_{\infty 2}}{\sigma_{nec} + (\theta^2 - 1)\Delta \beta_\infty} \right)^{1/2},$$

where $(\theta^2 - 1)\Delta = \gamma_1/\Gamma > 0$,

$$\bar{\phi} = \sigma_{nec} \left\{ \left(1 - \frac{\tilde{\sigma}}{\sigma_{nec}} \right) \left(1 - \frac{\beta_\infty}{\tilde{\beta}} \right) + \frac{3\lambda}{\sigma_{nec}} \right\},$$

and, as for the inhibitor-free case, $\sigma_\infty \sim \sigma_{nec} + \epsilon^2 \sigma_{\infty 2}$. The following expression for β_{nec} completes the solution:

$$\frac{\beta_{nec}}{\beta_\infty} \sim 1 - \frac{\delta^2 \theta^2}{2} (\eta_1 - \zeta_1)^2.$$

In this case, with $\lambda \sim O(1)$, the presence of the inhibitor has no effect on the tumour's growth: the rate of shrinkage of both η and ζ is still determined by λ. However, the reduction in the width of the proliferating rim which occurs when $\beta > 0$ corresponds to a reduction in the number of viable, or proliferating, cells and, hence, we conclude that the tumour poses less of a threat to its host.

Reducing the rate of necrosis, so that $\lambda = \delta\bar{\lambda}$, leaves the above expressions for $\eta - \zeta$, σ_∞ and β_{nec} unchanged whereas the expression for η becomes:

$$\eta \sim \eta_0(0) + \delta s \sigma_{nec} \left\{ \left(1 - \frac{\tilde{\sigma}}{\sigma_{nec}}\right)\left(1 - \frac{\beta_\infty}{\tilde{\beta}}\right)(\eta_1 - \zeta_1) - \frac{\bar{\lambda}\eta_0(0)}{\sigma_{nec}} \right\} t.$$

Now, provided that $(\sigma_{nec} - \tilde{\sigma})(\beta_\infty - \tilde{\beta}) > 0$, regression is predicted for all values of $\eta_0(0)$. In particular, if $\tilde{\sigma} < \sigma_{nec}$ and $\beta_\infty > \tilde{\beta}$ then the inhibitor actively initiates shrinkage of the tumour (compare figures 4 and 5(c)). When $(\sigma_{nec} - \tilde{\sigma})(\beta_\infty - \tilde{\beta}) < 0$ then, as for the inhibitor-free case, the tumour evolves to a stable configuration, for which the outer tumour radius η^{**} is given by:

$$\eta^{**} = \frac{\sigma_{nec}}{\bar{\lambda}}\left(1 - \frac{\tilde{\sigma}}{\sigma_{nec}}\right)\left(1 - \frac{\beta_\infty}{\tilde{\beta}}\right)\left(\frac{2\sigma_{\infty 2}}{\sigma_{nec} + \gamma_1\beta_\infty/\Gamma}\right)^{1/2}.$$

From the analysis presented above we note that if $\sigma_{nec} > \tilde{\sigma}$ and $\tilde{\beta} > \beta_\infty$ then presence of the inhibitor gives rise to a smaller tumour (see figure 5(a)) and that increasing the factor $\gamma_1\beta_\infty/\Gamma$ reduces both the equilibrium tumour radius η^{**} and the width of the proliferating rim. The detrimental action of the inhibitor predicted in table 3 and figures 5(b,c) can also be explained. If $\tilde{\sigma} > \sigma_{nec}$ then regression of the tumour is predicted when $\beta = 0$ whereas the inhibitor enables the system to support a stable, nontrivial tumour configuration when $\beta_\infty > \tilde{\beta}$.

6. Conclusions

In this paper we have developed and extended the previous work of [16] to include the growth of tumours which possess a central necrotic core. The analysis of this paper has enabled us to contrast the roles of apoptosis and necrosis and we have shown that whichever is the dominant cell loss mechanism depends on the tumour's size and structure. For example, in the case of a small necrotic core, apoptosis dominates, whereas for the thin proliferating rim, if $\lambda \sim O(1)$ then necrosis dominates and tumour regression results. In the special case $0 < \lambda \ll 1$, the existence of a stable, nontrivial solution with a thin proliferating rim is predicted.

In addition to providing insight into the roles of apoptosis and necrosis, the model enabled us to compare the action of a range of inhibitory mechanisms on the tumour's growth. Thus the inhibitor can be regarded as either an anti-cancer drug or a naturally-occurring inhibitor, stimulated by the immune system in response to the foreign body. Further the inhibitor may act either directly, by reducing the cell proliferation rate, or indirectly, by reducing the nutrient concentration.

Numerical simulations of the model, in the absence of any inhibitor ($\beta = 0$), exhibit two characteristic modes of tumour growth: either the tumour shrinks in size, and eventually disappears, or it evolves to a nonzero configuration which may possess a necrotic core (see figures 1(a)-(c)). From the simulations we observe that the type of behaviour which results is strongly influenced by the relative sizes of $\tilde{\sigma}, \sigma_{nec}$ and σ_∞. For example, with σ_∞ and σ_{nec} fixed, as $\tilde{\sigma}$ decreases, decay of the tumour to zero is superceded first by evolution of the tumour to a non-necrotic configuration for moderate values of $\tilde{\sigma}$ and to a necrotic configuration for smaller values of $\tilde{\sigma}$ (see figure 4).

Modifications to the tumour's growth characteristics may be effected by adapting the functional form of the proliferation rate and by introducing an inhibitor into the system. For example, using a logistic proliferation rate the appearance of an unstable nontrivial steady solution, having radius R_U say, is concomitant with the creation of a finite basin of attraction for the trivial solution: if the tumour radius is initially smaller than R_U then the tumour disappears; otherwise the tumour evolves to a necrotic configuration (see figure 2). Similarly, qualitative differences in the solution structure of the model may result from the inclusion of an inhibitor in the model (see figures 5(a)-(c)).

In order to complement the numerical results described above, analytical techniques were used to derive results for cases of physical interest which could be validated experimentally. In particular, it is possible to prove that if the rate of apoptosis is sufficiently large (here, $\tilde{\sigma} > \sigma_\infty$) then, in the absence of any inhibitor, no nontrivial solutions can occur and the tumour-free state persists. Also, directly after the onset of necrosis ($0 < r_{in} \ll 1$) the outer tumour radius R remains approximately constant and the balance between $\tilde{\sigma}$ and σ_{nec} determines the viability of the necrotic core. In particular, if $\tilde{\sigma} < \sigma_{nec}$ then the necrotic core expands rapidly until an equilibrium solution, with $r_{in} > 0$, is attained. Necessary conditions for the existence of tumours which possess the thin proliferating rim characteristic of multicellular spheroids are also derived. The dependence of the width of the proliferating rim on σ_∞ and σ_{nec}, as predicted from the asymptotic analysis, agrees with the expression assumed by Greenspan [4]. By focussing on such asymptotic limits, it is also possible to assess whether a given mode of inhibitor acts beneficially, reducing the tumour's size.

The results discussed above derive from an admittedly simple model of tumour growth, with scope for refinements. One simple extension to the model would be to examine the effect of asymmetric variations in the dependent variables: this is the subject of work in progress [26]. We remark that in our model no mention is made of the hypoxic, or non-proliferating, cell population which is known to play a major role in the success or failure of radiotherapy. In a well-developed, multi-layer tumour, radiotherapy typically targets and kills the proliferating cells located in the outer rim. This leads to recruitment of quiescent cells back into the proliferating regime. In particular, if a tumour possesses a large quiescent population then, after treatment, it may recommence growing, possibly exceeding its pre-radiotherapy size. Whilst it would be relatively straightforward to include quiescence in our model, by extending the admissible tumour structures to say three layers, the complexity of the two-layer necrotic model discussed in this paper suggests that such generalisations would be of limited use since similar analysis would be rendered intractable. Given the importance of the functional form of the proliferation rate on the qualitative behaviour of the tumour, it seems particularly important to employ experimentally determined expressions interaction terms such as $S(\sigma, \beta)$. The decision to employ simpler expressions here was taken in order to focus on a methodological approach for studying tumour growth, which can be easily adapted to a particular situation. Whilst any modifications would, in general, necessitate numerical simulations, we believe that, by demonstrating the existence and stability of nontrivial tumours for our simplistic model, some insight into the generic behaviour of tumours can be derived.

We now discuss the practical implications of the results derived above. The asymptotic analysis could be used in conjunction with experimental data from multicellular spheroids to estimate system parameters. For example, data tracking the evolution of the outer tumour radius and the necrotic radius could by used to validate the claim made in section 5.1 that, directly after the onset of necrosis, the necrotic core grows more rapidly than the outer tumour radius. Such data could also be used to estimate the ratio $\tilde{\sigma}/\sigma_{nec}$ and to assess the viability of the necrotic core. Data describing the limiting, or equilibrium, tumour radii could be used to verify the claim that a necessary condition for the existence of thin proliferating rims is that σ_∞ and σ_{nec} are approximately equal and that, in this case, $R - r_{in} \propto (\sigma_\infty - \sigma_{nec})^{1/2}$. Modifications to the limiting tumour radii affected by the addition of a prospective anti-cancer drug could also be used, in tandem with the inhibitor-present extension of the thin proliferating rim analysis, to assess the tumour's handling of the drug. For example the results of section 5.2 could be used to estimate γ_1/Γ, the relative rate at which the inhibitor degrades the nutrient relative to its natural decay

More generally, given the interpretations of the inhibitor species as an immune response or an anticancer drug, the numerical simulations of sections 3 and 4 provide some insight into the way in which failure of the immune response can induce cancers (inhibitor as immune response) and also why similar patients respond differently to the same treatment (inhibitor as anticancer drug). For example, from table 2 we conclude that whilst one patient may respond favourable to treatment another patient, having different 'parameter values', may deteriorate when given the same treatment. The results presented in figures 5(a,b,c) further demonstrate how the intricate balance between the different physical processes affects the viability of a tumour and highlights the difficulties associated with prescribing anticancer drugs to patients. For example, the inhibitor considered in figure 5(a) merely reduces the size of the tumour, without eliminating it. By contrast the inhibitor shown in figure 5(c) eliminates those tumours which would persist in the absence of the inhibitor. However, treatment with this chemical runs the risk of inducing tumours in parts of the body for which $\tilde{\sigma} > \sigma_\infty$. The appearance of multiple steady state solutions in tables 1 and 2 and figure 5(b,c), and the concomitant stabilisation of the trivial, tumour-free state, further emphasises the need for accurate monitoring of patients during treatment. In this case, a patient with two tumours of different sizes, treated with an anticancer drug may find that whilst the smaller, less harmful tumour disappears the larger one actually grows in size.

Bibliography

[1] J.A. Adam, A mathematical model of tumour growth. II. Effects of geometry and spatial uniformity on stability, *Math. Biosci.* 86:183-211 (1987).

[2] J.A. Adam, A mathematical model of tumor growth III: Comparison with experiment, *Math. Biosci.* 86:213-227 (1987).

[3] J.A. Adam and S.A. Maggelakis, Diffusion regulated growth characteristics of a spherical prevascular carcinoma, *Bull. M. Bio.* 52:549-582 (1990).

[4] H.P. Greenspan, Models for the growth of a solid tumour by diffusion, *Stud. Appl. Math.* 52:317-340 (1972).

[5] S.A. Maggelakis and J.A. Adam, Mathematical model of prevascular growth of a spherical carcinoma, *Math. Comput. Modelling* 13:23-38 (1990).

[6] G. Adam, U. Steiner, H. Maier and S. Ulrich, Analysis of cellular interactions in density-dependent inhibition of 3T3 cell proliferation, *Biophys. Struct. Mech.* 9:75-82 (1982).

[7] J.P. Freyer and R.M. Sutherland, Regulation of growth saturation and development of necrosis in EMT6/Ro multicellular spheroids by the glucose and oxygen supply, *Cancer Res.* 46:3504-3512 (1986).

[8] J.P. Freyer and R.M. Sutherland, Proliferative and clonogenic heterogeneity of cells from EMT6/Ro multicellular spheroids induced by the glucose and oxygen supply, *Cancer Res.* 46:3513-3520 (1986).

[9] R.M. Sutherland and R.E. Durand, Radiation response of multicell spheroids - an in vitro tumour model, *Internat. J. Radiat. Biol.* 23:235-246 (1973).

[10] R.M. Sutherland and R.E. Durand, Growth and cellular characteristics of multicell spheroids, *Recent Results in Cancer Research* 95:24-49 (1984).

[11] R.M. Sutherland, Cell and environment interactions in tumor microregions: the multicell spheroid model, *Science* 240:177-184 (1988).

[12] M. Tubiana, The kinetics of tumour cell proliferation and radiotherapy, *Br. J. Radiol.* **44**, 325-347 (1971).

[13] O.H. Iversen, Epidermal chalones and squamous cell carcinomas *Virchows Arch. B Cell Path.* 27:229-235 (1978)

[14] O.H. Iversen, The Chalones, in: *Tissue Growth Factors* (Ed. Baserga, R.) pp. 491-550 (1981) Berlin:Springer-Verlag.

[15] O.H. Iversen, What's new in endogenous growth stimulators and inhibitors (chalones), *Path. Res. Pract.* 180:77-80 (1985).

[16] H.M. Byrne and M.A.J. Chaplain, Growth of non-necrotic tumours in the presence and absence of inhibitors, *Math. Biosci.* (in press) (1995).

[17] J.F.R. Kerr, Shrinkage necrosis; a distinct mode of cellular death, *J. Path.* 105:13-20 (1971).

[18] J.F.R. Kerr, A.H. Wyllie and A.R. Currie, Apoptosis: a basic biological phenomenon with wide-ranging implications in tissue kinetics, *Br. J. Cancer* 26:239-257 (1972).

[19] D.L.S. McElwain and L.E. Morris, Apoptosis as a volume Loss mechanism in mathematical models of solid tumour growth, *Math. Biosci.* 39:147-157 (1978).

[20] R.E. Durand, Cell cycle kinetics in an *in vitro* tumour model, *Cell Tissue Kinet.* 9:403-412 (1976).

[21] R.E. Durand, Multicell spheroids as a model for cell kinetic studies, *Cell Tissue Kinet.* 23:141-159 (1990).

[22] M.A.J. Chaplain and N.F. Britton, On the concentration profile of a growth inhibitory factor in multicell spheroids, *Math. Biosci* 115:233-245 (1993).

[23] D.L.S. McElwain and P.J. Ponzo, A model for the growth of a solid tumor with non-uniform oxygen consumption, *Math. Biosci.* 35:267-279 (1977).

[24] J. Folkman and M. Hochberg, Self-regulation of growth in three dimensions, *J. Exp. Med.* 138:745-753 (1973).

[25] M.H. Protter and H.F. Weinberger, *Maximum principles in differential equations*, Springer-Verlag, New York, 1984.

[26] H.M. Byrne and M.A.J. Chaplain, On the growth and stability of avascular tumours subjected to asymmetric perturbations (in preparation), 1995.

List of Legends for Diagrams

Figure 1(a): Evolution of η and ζ when $\beta = 0$, $S(\sigma, \beta) = s(\sigma - \tilde{\sigma})$. All initial data converge to the limiting values $\eta^{\infty} \sim 2.42$ and $\zeta \sim 0.63$. Key: $\eta(t)$ '—'; $\zeta(t)$ '- - -'. Parameter values: $\sigma_{\infty} = 0.8, \sigma_{nec} = 0.4, \tilde{\sigma} = 0.5, \lambda = 0.1, \Gamma = 25, s = 100$. Initial scaled tumour radius: $\eta(0) = \sqrt{\Gamma} = 5.0$.

Figure 1(b): Evolution of η and ζ when $\beta = 0$, $S(\sigma, \beta) = s(\sigma - \tilde{\sigma})$ and the rate of apoptosis is increased to $\tilde{\sigma} = 0.7$. All initial data converge to a non-necrotic tumour for which $\eta^{\infty} \sim 1.51$ and $\zeta = 0.00$. Key: $\eta(t)$ '—'; $\zeta(t)$ '- - -'. Parameters values are as per figure 1(a), except $\tilde{\sigma} = 0.7$.

Figure 1(c): Evolution of η and ζ when $\beta = 0$, $S(\sigma, \beta) = s(\sigma - \tilde{\sigma})$ and the rate of apoptosis is increased to $\tilde{\sigma} = 0.9$. All initial data converge to the trivial case for which $\eta^{\infty} = 0.00 = \zeta$. Key: $\eta(t)$ '—'; $\zeta(t)$ '- - -'. Parameters values are as per figure 1(a), except $\tilde{\sigma} = 0.9$.

Figure 2: Evolution of η and ζ when $\beta = 0$, $S(\sigma, \beta) = s\sigma(1 - \sigma/\hat{\sigma})$, showing decay of the tumour to zero if $\eta(0) < 2.2$ and growth to a nontrivial configuration otherwise. Key: $\eta(t)$ '—'; $\zeta(t)$ '- - -'. Parameter values: $\sigma_{\infty} = 0.8, \sigma_{nec} = 0.4, \hat{\sigma} = 0.64, \lambda = 0.1, \Gamma = 25, s = 100$.

Figure 3: Evolution of η when $\beta > 0$ and $S(\sigma, \beta) = s(\sigma - \tilde{\sigma})(1 - \beta/\tilde{\beta})$ showing decay of the tumour to zero if $\eta(0) < 0.98$ and convergence to a nontrivial configuration otherwise. Parameter values: $\sigma_{\infty} = 0.8, \sigma_{nec} = 0.4, \tilde{\sigma} = 0.2, \beta_{\infty} = 1.0, \tilde{\beta} = 0.9, \lambda = 0.1, \gamma_1 = 0.8, \gamma_2 = 2.0, \Gamma = 25.0, s = 100$.

Figure 4: Dependence of the steady-state scaled tumour radii on the rate of apoptosis, $\tilde{\sigma}$, when $\beta = 0$ and $S(\sigma, \beta) = s(\sigma - \tilde{\sigma})$. The existence of necrotic and non-necrotic tumours is restricted to a finite range of $\tilde{\sigma}$. Key: η '—'; ζ '- - -'. Parameter values: $\sigma_{\infty} = 0.8, \sigma_{nec} = 0.4, \lambda = 0.1$.

Figure 5(a): The effect on the scaled steady-state tumour radii of an inhibitor species ($\beta > 0$) is compared with the inhibitor-free situation ($\beta \equiv 0$) as $\tilde{\sigma}$ varies. The inhibitor acts both directly, via the cell proliferation rate, and indirectly, consuming the nutrient species. In this case, the inhibitor simply reduces the size of the nontrivial, inhibitor-free tumour radii. Key: inhibitor-present tumour radii '—–'; inhibitor-free tumour radii '- - -'. Parameter values: $\sigma_\infty = 0.8, \sigma_{nec} = 0.4, \lambda = 0.1, \beta_\infty = 1.0, \tilde{\beta} = 5.0, \gamma_1 = 0.8, \gamma_2 = 2.0$.

Figure 5(b): The effect on η and ζ of increasing the strength of the direct inhibitor action ($\tilde{\beta} = 0.9$). In this case, when $\tilde{\sigma} < \sigma_\infty$ the existence of nontrivial solutions is restricted to a smaller range of $\tilde{\sigma}$ than for the inhibitor-free case. However, where they exist these solutions are nonunique. In addition, the existence of non-necrotic solutions is predicted when $\tilde{\sigma} > \sigma_\infty$. Key: η '—–'; ζ '- - -'. Parameter values: $\sigma_\infty = 0.8, \sigma_{nec} = 0.4, \lambda = 0.1, \beta_\infty = 1.0, \tilde{\beta} = 0.9, \gamma_1 = 0.8, \gamma_2 = 2.0$.

Figure 5(c): The effect on η and ζ of increasing the strength of the direct inhibitor action even further ($\tilde{\beta} = 0.5$). In this case the existence of nontrivial solutions is confined to the range $\tilde{\sigma} > 0.6$, with the interval $0 < \tilde{\sigma} < 0.6$ now being a tumour-free region. Key: η '—–'; ζ '- - -'. Parameter values: $\sigma_\infty = 0.8, \sigma_{nec} = 0.4, \lambda = 0.1, \beta_\infty = 1.0, \tilde{\beta} = 0.5, \gamma_1 = 0.8, \gamma_2 = 2.0$.

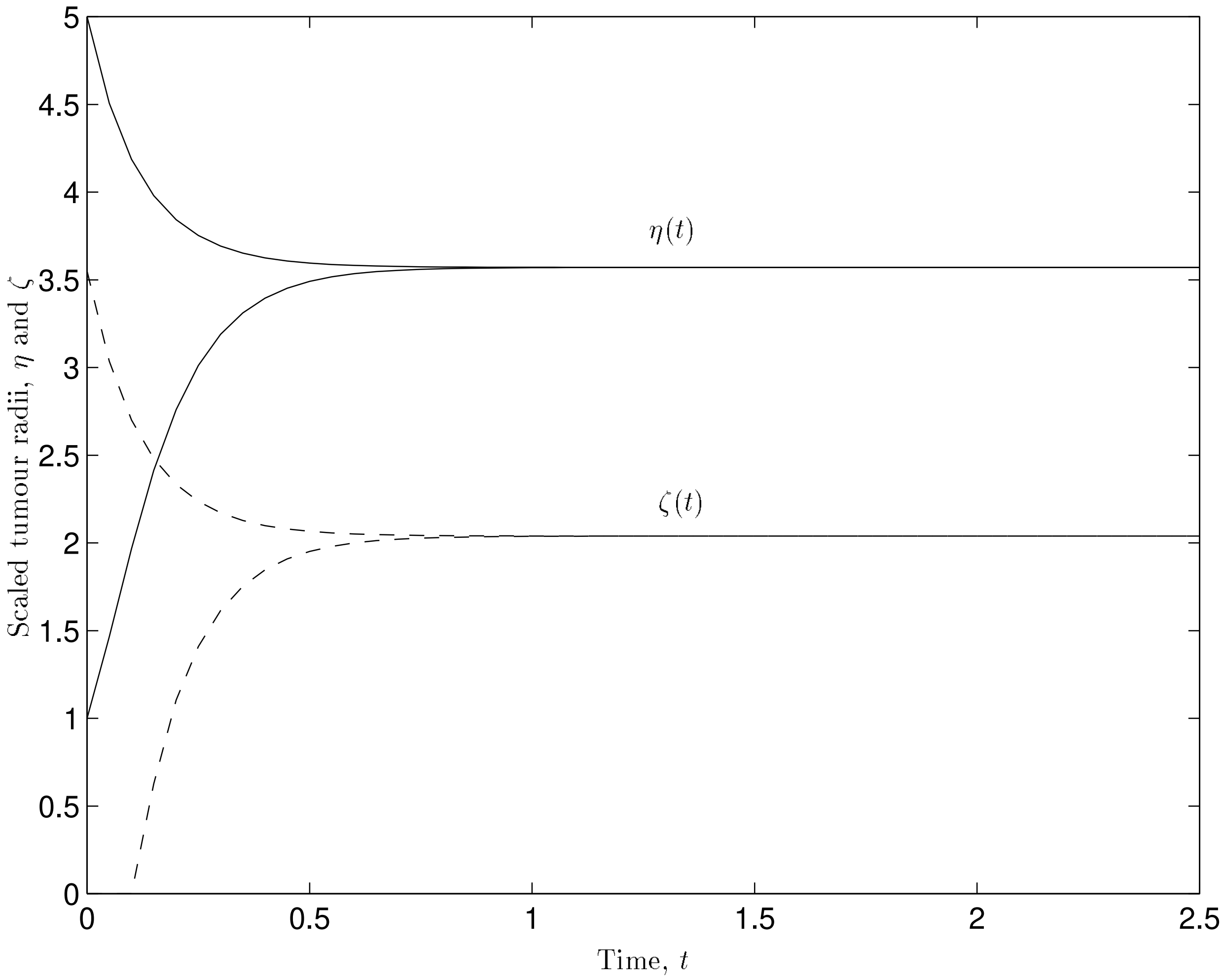

Byrne & Chaplain: Figure 1(a)

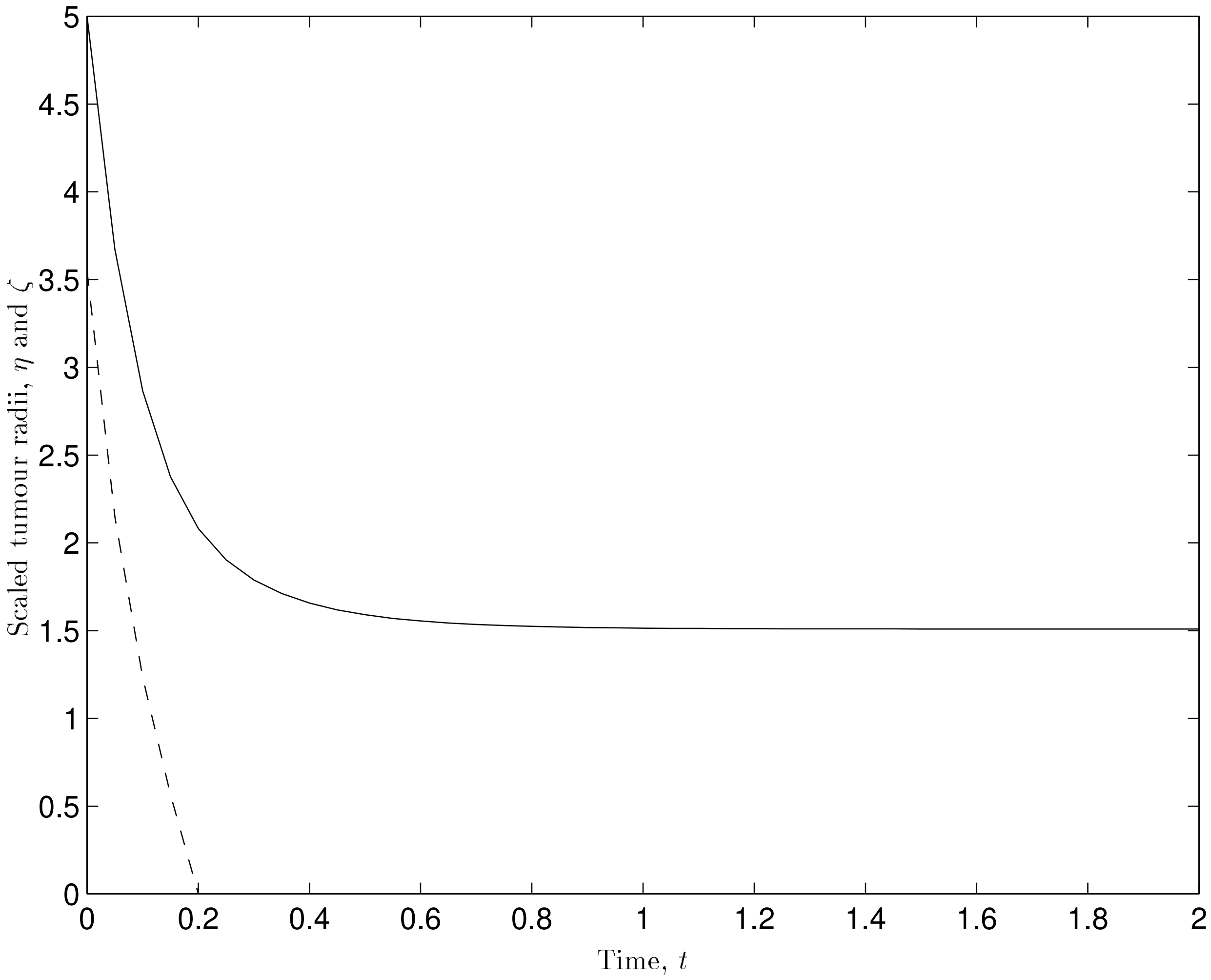

Byrne & Chaplain: Figure 1(b)

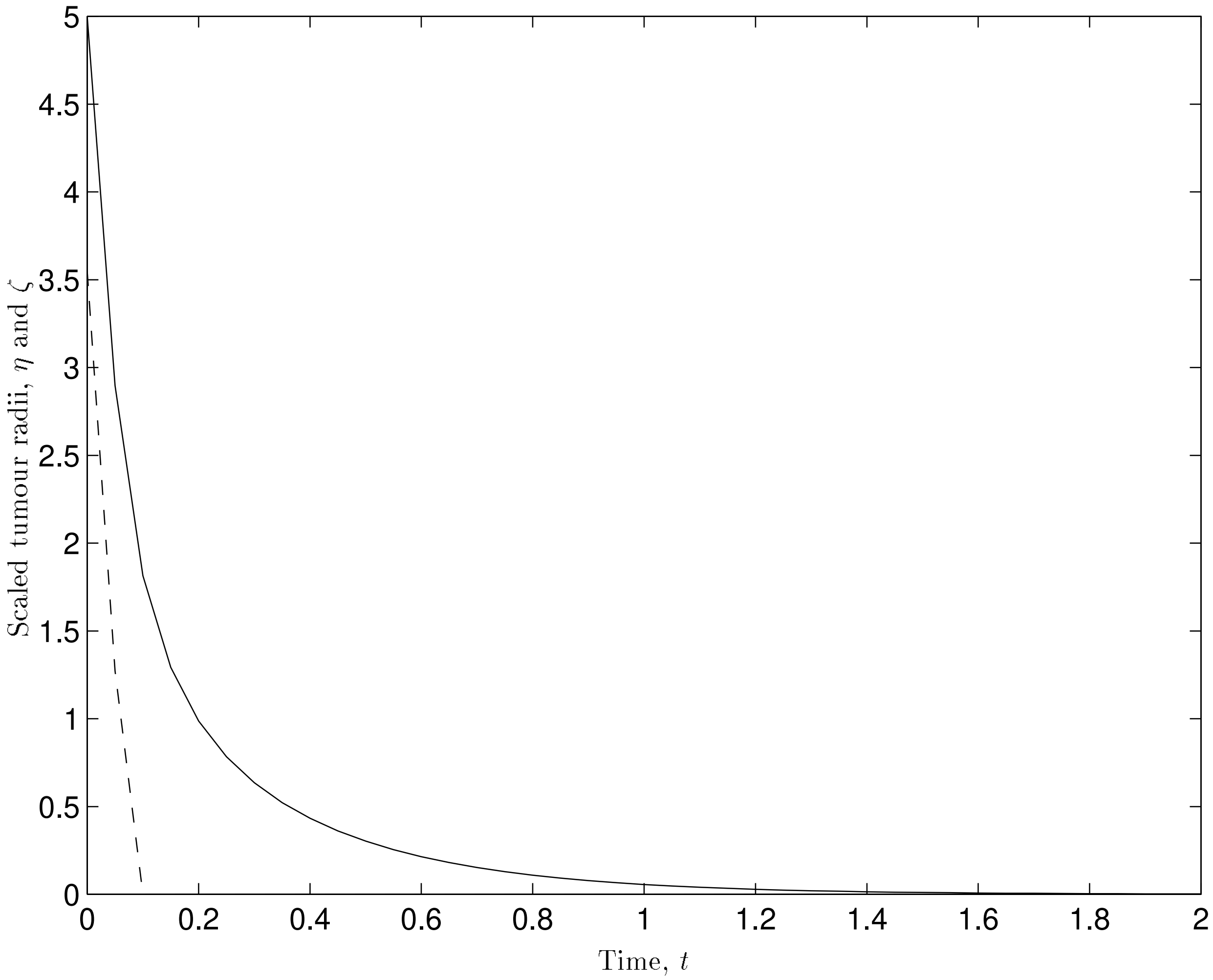

Byrne & Chaplain: Figure 1(c)

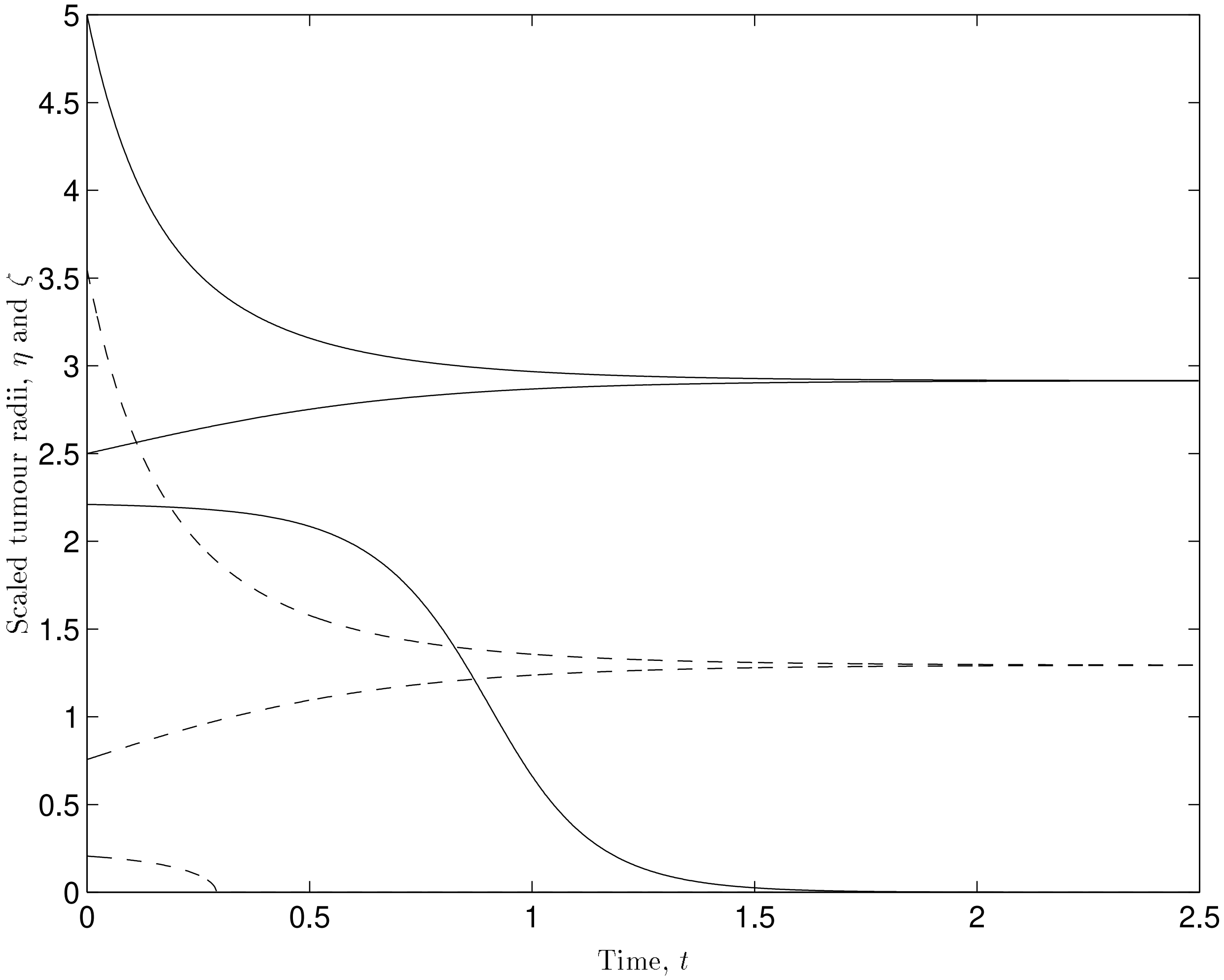

Byrne & Chaplain: Figure 2

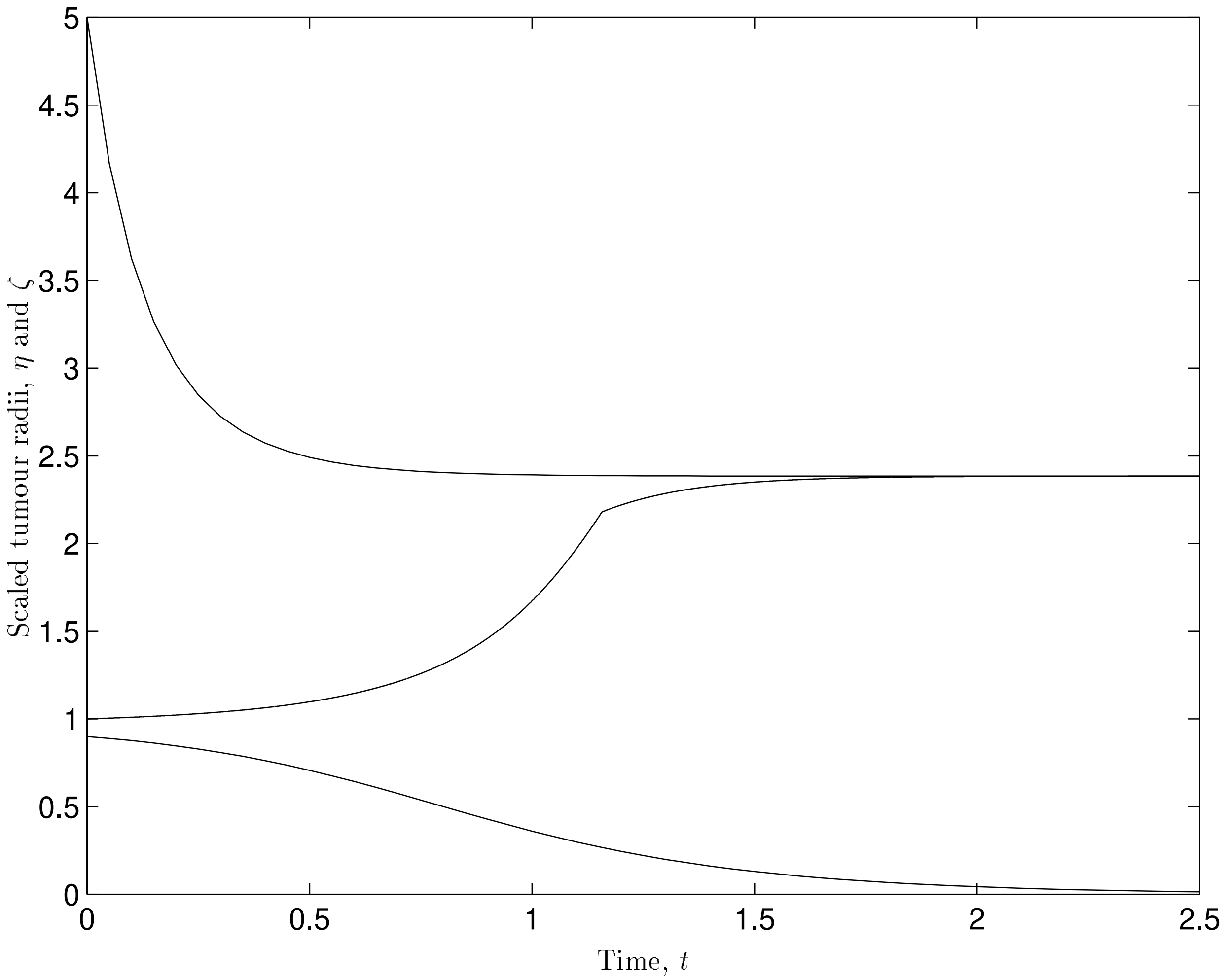

Byrne & Chaplain: Figure 3

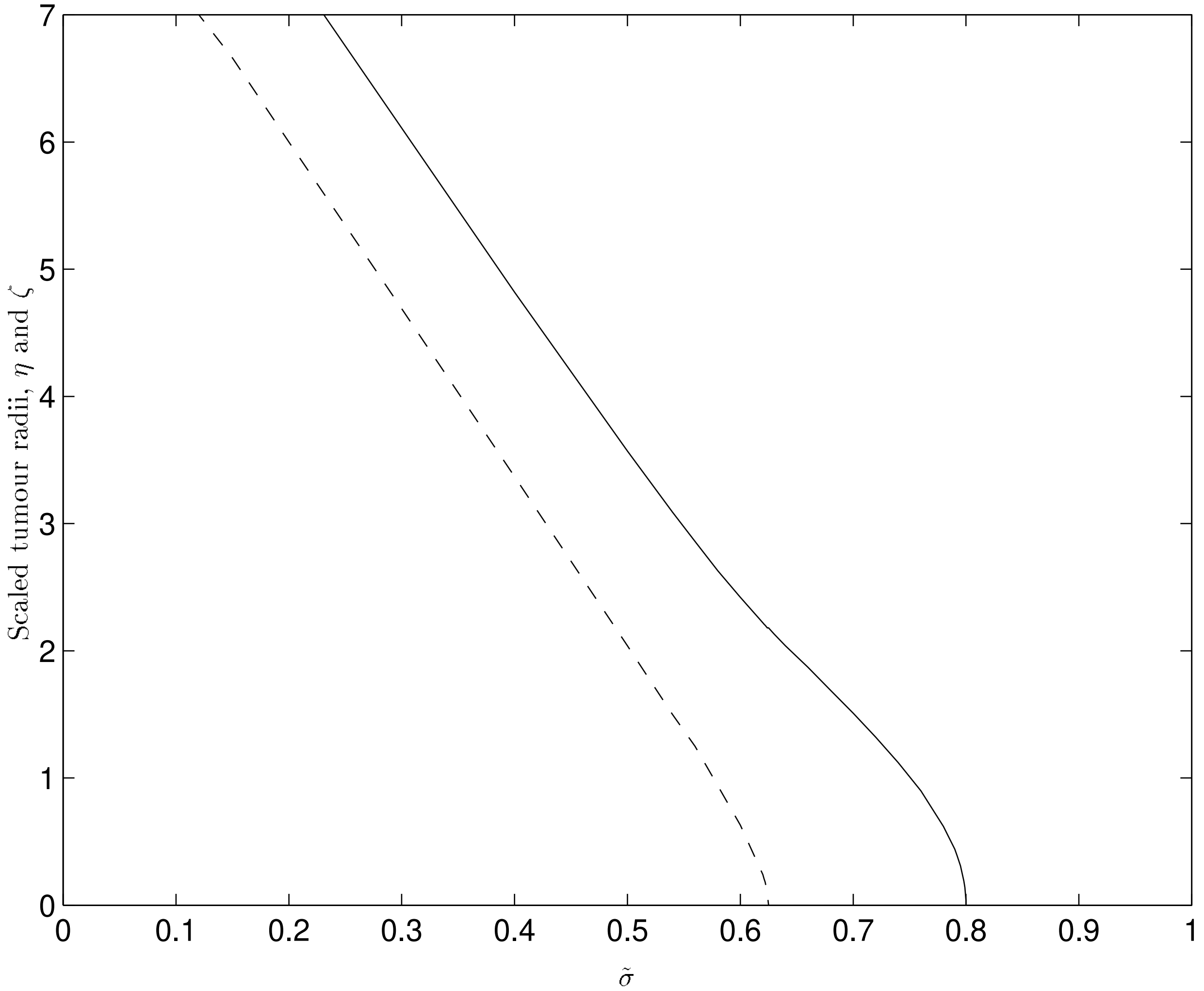

Byrne & Chaplain: Figure 4

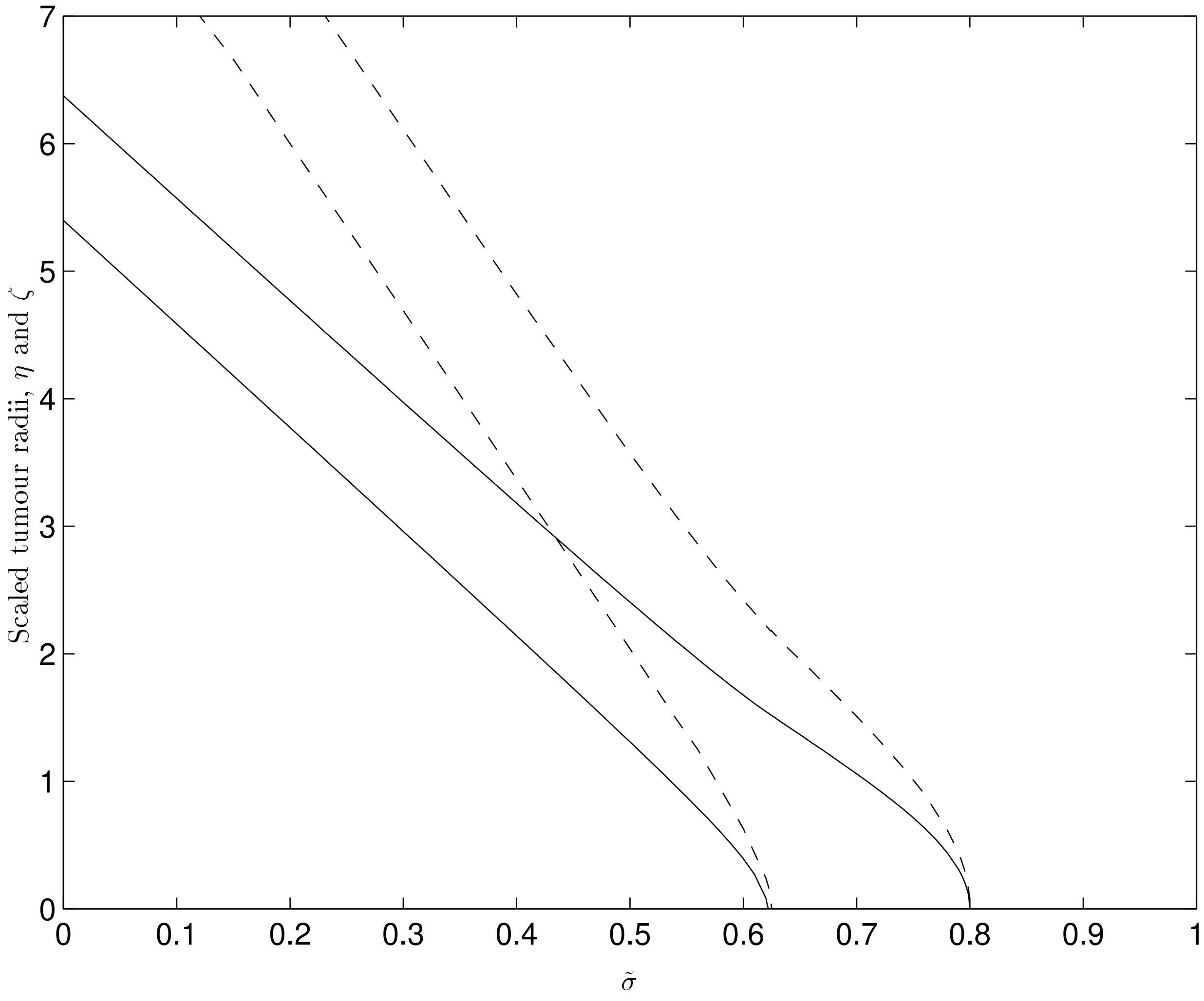

Byrne & Chaplain: Figure 5(a)

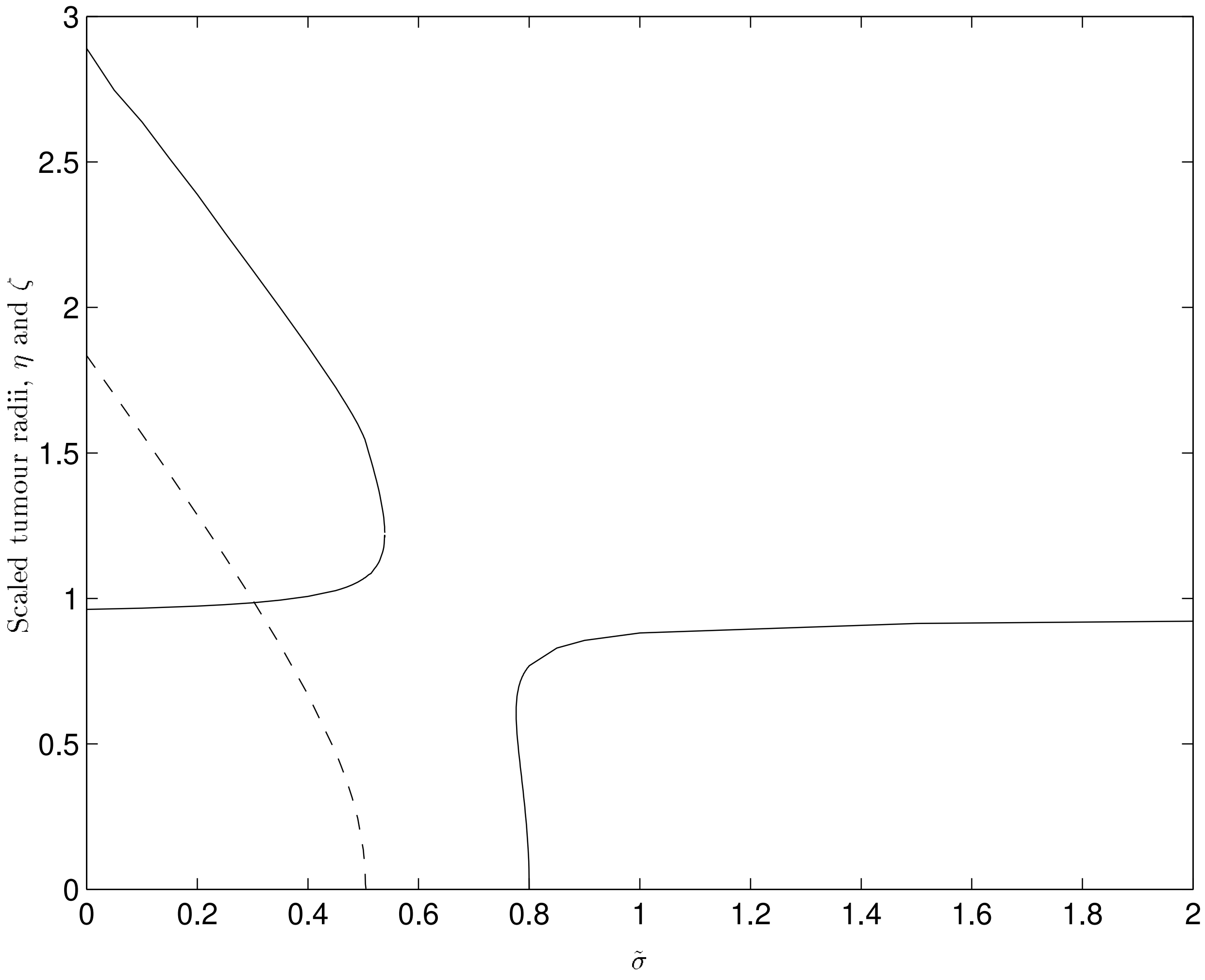

Byrne & Chaplain: Figure 5(b)

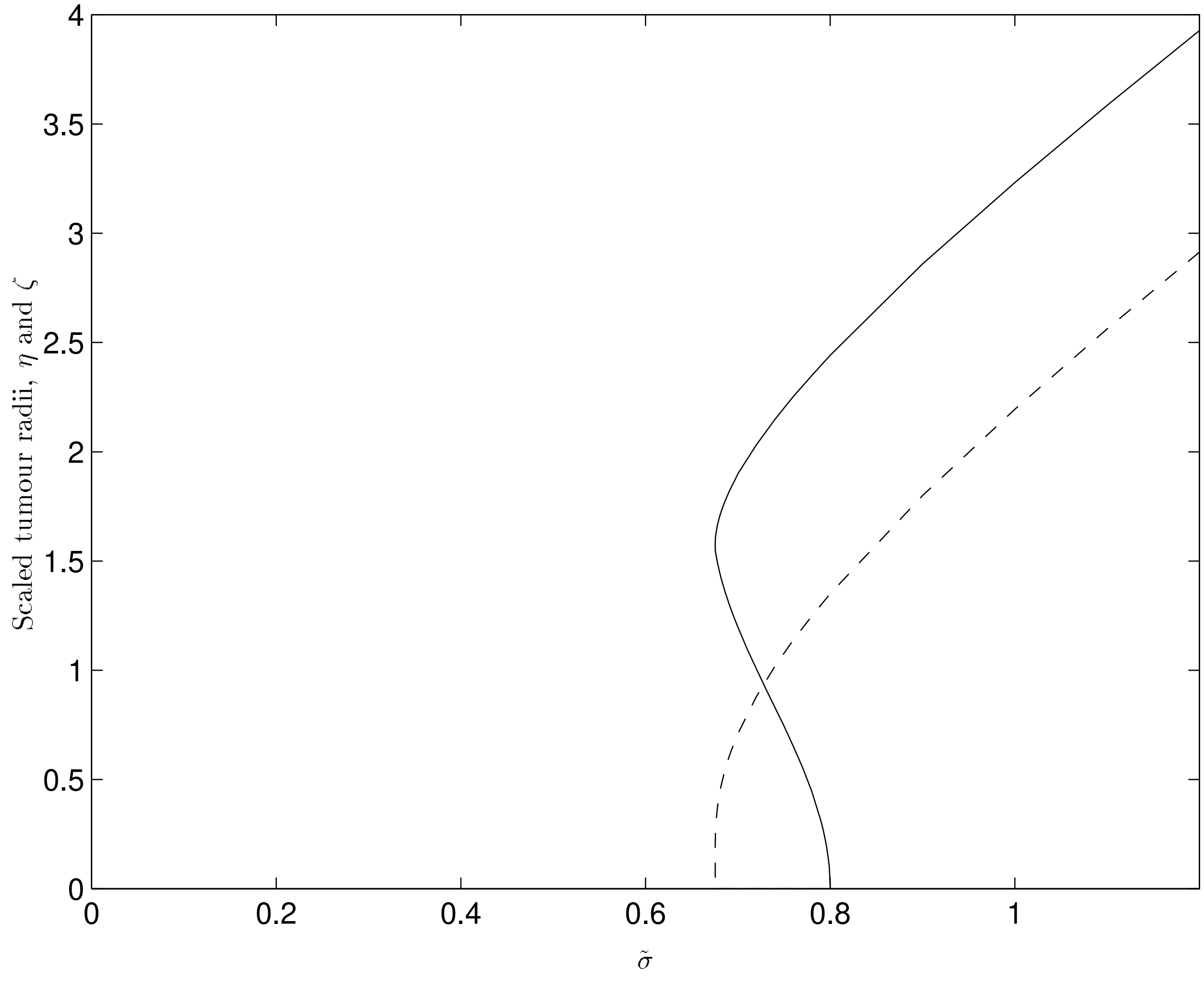

Byrne & Chaplain: Figure 5(c)